DESIGN AND INVESTIGATE THE MANUAL SUN TRACKING SYSTEM

‘IMRAN BIN AHMAD ROSDI

BACHELOR OF ENGINEERING
UNIVERSITY MALAYSIA PAHANG

2012

UNIVERSITI MALAYSIA PAHANG

BORANG PENGESAHAN STATUS TESIS

JUDUL: <u>DESIGN AND INVESTIGATE THE MANUAL SUN TRACKING SYSTEM</u>

SESI PENGAJIAN: <u>2011/2012</u>

Saya, **<u>‘IMRAN BIN AHMAD ROSDI (890914-14-5191)</u>**

mengaku membenarkan tesis (Sarjana Muda / ~~Sarjana / Doktor Falsafah~~)* ini disimpan di perpustakaan dengan syarat-syarat kegunaan seperti berikut:

1. Tesis ini adalah hakmilik Universiti Malaysia Pahang (UMP).
2. Perpustakaan dibenarkan membuat salinan untuk tujuan pengajian sahaja.
3. Perpustakaan dibenarkan membuat salinan tesis ini sebagai bahan pertukaran antara institusi pengajian tinggi.
4. **Sila tandakan (√)

	SULIT	(Mengandungi maklumat yang berdarjah keselamatan atau kepentingan Malaysia seperti yang termaktub di dalam AKTA RAHSIA RASMI 1972)
	TERHAD	(Mengandungi maklumat TERHAD yang telah ditentukan oleh organisasi / badan di mana penyelidikan dijalankan)
√	**TIDAK TERHAD**	

Disahkan oleh:

(TANDATANGAN PENULIS) (TANDATANGAN PENYELIA)

Alamat Tetap:

<u>NO 282 JALAN H2,</u>
<u>FASA 5, TAMAN MELAWATI</u>,
<u>53100 KUALA LUMPUR</u>.
Tarikh: **<u>25 JUNE 2012</u>**

<u>Mr LEE GIOK CHUI</u>
(Nama Penyelia)

Tarikh: **<u>25 JUNE 2012</u>**

CATATAN: * Potong yang tidak berkenaan.

** Jika tesis ini SULIT atau TERHAD, sila lampirkan surat daripada pihak berkuasa/organisasi berkenaan dengan menyatakan sekali tempoh tesis ini perlu dikelaskan sebagai SULIT atau TERHAD.

◆ Tesis dimaksudkan sebagai tesis bagi Ijazah Doktor Falsafah dan Sarjana secara Penyelidikan, atau disertasi bagi pengajian secara kerja kursus dan penyelidikan, atau Laporan Projek Sarjana Muda (PSM).

DESIGN AND INVESTIGATE THE MANUAL SUN TRACKING SYSTEM

‘IMRAN BIN AHMAD ROSDI

Report submitted in fulfillment of the requirements
for the award of the degree of
Bachelor of Mechanical Engineering

Faculty of Mechanical Engineering
UNIVERSITI MALAYSIA PAHANG

JUNE 2012

UNIVERSITI MALAYSIA PAHANG

FACULTY OF MECHANICAL ENGINEERING

I certify that the project entitled “Design and Investigate The Manual Sun Tracking System” is written by ‘Imran Bin Ahmad Rosdi. I have examined the final copy of this project and in our opinion, it is fully adequate in terms of scope and quality for the award of degree of Bachelor Engineering. I herewith recommend that it be accepted in partial fulfillment of the requirements for the degree of Bachelor of Mechanical Engineering.

(Mr. RosmaziRosli)

Examiner Signature

SUPERVISOR'S DECLARATION

I hereby declare that I have checked this project and in my opinion, this project is adequate in terms of scope and quality for the award of the degree of Bachelor of Mechanical Engineering.

Signature :

Name of Supervisor : Mr. Lee Giok Chui SMN, KMN.

Position : LECTURER

Date : 22 June 2012

STUDENT'S DECLARATION

I declare that this report titled "Design and Investigate The Manual Sun Tracking System" is my result of my own research except as stated in the references. The project has not been accepted for any degree and is not concurrently submitted for award of other degree.

Signature :

Name : 'IMRAN BIN AHMAD ROSDI

ID Number : MA08072

Date : 22 June 2012

Dedicated, truthfully for supports,

encouragements and always be there during hard times,

to my beloved family

ACKNOWLEDGEMENT

First of all, I would like to express my highest gratitude to Allah the Almighty for blessing me in finishing this project. Besides, I would like to take this opportunity to express my sincere gratitude and appreciation especially to my supervisor, Mr.Lee Giok Chui for his constant guidance, consideration and constructive idea in leading me to accomplish this project.Thanks a lot for giving me a professional training, advice and suggestion to bring this thesis to its final form. Without his support and interest, this thesis would not have been the same as presented here. I am very grateful for his patience and his constructive comments that enriched this research project.

Besides that, I would like to acknowledge with much appreciation the crucial role of the staff in the Faculty of Mechanical Engineering, for their valuable comments, sharing their time and knowledge on this research project during the project was carried out and giving a permission to use all the necessary tools in the laboratory. They have contributed towards my understanding and thoughts.

Last but not least, an expression of thanks is extended to everyone who has offered their help and support especially to my family and friends. All of their helps are very significant to the success of this project. I cannot find the appropriate words that could properly describe my appreciation for their devotion, support and faith in my ability to attain my goal.

ABSTRACT

According to market economy, the increasing worldwide demand for energy has continuously forces a rise on the price of fossil combustibles. In fact, the demand for energy is expected to grow faster than the finding out of new available fossil resources in the near future. The sun or solar energy had been identified as the most powerful energetic power source in our planet and it is expected that the sun will become the main electricity production source. The solar energy distribution is more depended on the position of the panel and the sun location. This project is about designing and analyzing the manual sun tracking system that can follow the sun movement. The objectives for this project are to design and analyze the single axis sun tracking system for flat plate solar collector. This project involves designing five main part of the manual sun tracking system which is frame, base, link, crank and pin. The analysis is done using SolidWorksSimulationXpress, ALGOR(FemPro) and Sam6.1. SolidWorksSimulationXpressis used to simulate and analyze the frame, base, link and crank part while ALGOR(FemPro) are used to simulate the designing part of pin. Sam6.2 is used to simulate and analyze the mechanism of the assembly design. All the designed part have safety factor more than one and are properly design and stable. However field test should be done to validate the final design and study the effect of the sun tracking system to solar collector.

ABSTRAK

Menurut kepada pasaran semasa, permintaan yang semakin meningkat di seluruh dunia terhadap tenaga terus memaksa kenaikan harga minyak fosil. Malah, dalam masa yang terdekat, permintaan untuk tenaga dijangka berkembang lebih cepat daripada mencari sumber fosil yang baru. Matahari atau tenaga solar telah dikenalpasti sebagai sumber kuasa yang paling kuat dalam planet ini dan dijangka bahawa matahari akan menjadi sumber utama pengeluaran elektrik. Taburan tenaga solar lebih bergantung kepada kedudukan panel dan lokasi matahari. Projek ini adalah untuk mereka bentuk dan menganalisis sistem manual penjejak matahari. Objektif bagi projek ini adalah untuk mereka bentuk dan menganalisis sistem penjejak satu paksi matahari untuk pengumpul suria rata. Projek ini melibatkan merekabentuk lima bahagian utama sistem penjejak matahari manual iaitu bingkai, tapak, link, engkol dan pin.. Kemudian analisis dilakukan dengan menggunakan SolidWorks SimulationXpress, ALGOR(FemPro) dan Sam6.2. SolidWorks SimulationXpress digunakan untuk mensimulasikan dan menganalisis bahagian bingkai, tapak, link dan engkol manakala ALGOR(FemPro) digunakan untuk mensimulasikan bahagian rekabentuk pin. Sam6.2 digunakan untuk mensimulasikan dan menganalisis mekanisme rekabentuk keseluruhan. Semua bahagian yang direka mempunyai faktor keselamatan lebih daripada satu dan direka bentuk dengan betul dan stabil. Walau bagaimanapun, kajian makmal perlu dilakukan untuk mengesahkan reka bentuk akhir dan mengkaji kesan sistem penjejak matahari kepada pengumpul suria rata.

TABLE OF CONTENTS

LIST OF TABLES

LIST OF FIGURES

LIST OF SYMBOLS

mm	Millimeter
d	Diameter
MPa	Mega Pascal
°	Degree
%	Percent
^{o}C	Degree Celsius
kN	Kilo Newton
m	Meter
min	Minutes
Mn	Manganese
C	Carbon
mm^2	Millimeter square
N	Newton
kg	Kilogram
m/s	Meter per second
ave	Average
σ_1	Stress on X-axis
σ_2	Stress on Y-axis
σ_3	Stress on Z-axis
F_s	Sheer Force
A	Area
τ	Sheer Stress
σ_b	Bearing Stress

F_b	Bearing Force
t	Thickness
σ'	Stress
F.S	Factor of Safety
S_y	Yield Point
τ_{max}	Maximum Sheer Stress
M	Bending Moment
I	Moment of Inertia
SR	Slenderness Ratio
L_{eff}	Effective Length
r	Radius
σ_{max}	Maximum Stress
σ_{ave}	Average Stress
K_t	Stress Concentration Factor
N/mm^2	Newton Per Millimeter Square
kg/m^2	Kilogram Per Meter Square
m^2	Meter Square
∅	Diameter

LIST OF ABBREVIATIONS

ASTM	American Society for Testing and Materials
ASME	American Society of Mechanical Engineers
MS	Malaysian Standard
AISI	American iron and steel institute
ANSI	American National Standards Institute
SENB	Single edge notch bending
SimulationExpresss	SolidWorks simulation software
FEA	Finite element analysis
Sam6.1	Mechanism design simulation software

CHAPTER 1

INTRODUCTION

1.1 PROJECT BACKGROUND

Today domestic homes, schools, businesses and even any building on earth all have the potential to utilize solar power to provide on-site free electricity or at lease to reduce demand for energy from the usual main energetic sources such as fossil combustibles(petroleum and gas). According to market economy, the increasing worldwide demand for energy has continuously forces a rise on the price of fossil combustibles. In fact, the demand for energy is expected to grow faster than the finding out of new available fossil resources in the near future (Khan, N 2007).

The sun or solar energy had been identified as the most powerful energetic power source in our planet and it is expected that the sun will become the main electricity production source (WBGU (German Advisory Council on Global Change) 2003).

The solar energy distribution is more depended on the position of the panel and the sun location. Mostly a typical household solar photovoltaic system are fixed on the sloping roof or on the framework fixed to the ground but the sun always moving across the sky through the day from east to the west. Solar panels are usually set up to directly facing the sun at the middle of the day where the maximum solar energy can be emitted. Therefore morning and evening sunlight hits the panel at an acute angle reducing the total amount of heat which can be collected. Thus the developing of flexible solar panel is very important.

1.2 PROJECT PROBLEM STATEMENT

The solar energy had been identified as the most powerful energy source but yet not fully developed. Solar panel that had been used at most houses are having low efficiency and not convenience to be used as main energy source. Solar energy until today had only been used as secondary energy source to reduce or back up other energy source.

A specific location on the earth will always receive the maximum amount of solar energy when the sun’s energy hits the surface directly. The further the panel moves away from the equator the greater the angle of incidence and therefore the less solar energy. Thus, it is important for the solar panel to face directly to the sun at most of the time.

1.3 PROJECT OBJECTIVE

The primary objective of this project is to design and analyze the model of the manual sun tracking system. In order to achieve the primary objective, this project was added with other objectives. The objectives are as follow:

i. To design the manual sun tracking system using available material.
ii. To investigate the strength of the structure.

1.4 PROJECT SCOPE

The project is divided to two parts which is design and investigates the model of the manual sun tracking system. The design process is done by using SolidWorks software. In order to design, the model is divided to a few parts. The parts were not divided just for designing purpose but also to make it easier to analyze. To investigate the strength of the structure SimulationXpress and ALGOR FemPro is used.

CHAPTER 2

LITERATURE REVIEW

2.1 INTRODUCTION

To perform this study, the understanding of the project is very important thus it is very relevant to study and analyze the literature. Journal, books, previous study and internet sources were used as the material.

2.2 SOLAR RADIATION

The Sun is the most prominent feature in our solar system. It is the largest object and contains approximately 98% of the total solar system mass. One hundred and nine Earths would be required to fit across the Sun's disk, and its interior could hold over 1.3 million Earths. The Sun's outer visible layer is called the photosphere and has a temperature of 6,000°C. This layer has a mottled appearance due to the turbulent eruptions of energy at the surface. The Sun's period of rotation at the surface varies from approximately 25 days at the equator to 36 days at the poles. Deep down, below the convective zone, everything appears to rotate with a period of 27 days. Solar radiation is energy emanating from the sun in the form of waves

2.2.1 Radiation

Energy that transfers through electromagnetic waves that travels at the speed of light. The velocity of light in a vacuum is approximately 3×10^8 m/s. The time it takes light from the sun to reach the Earth is 8 minutes and 20 seconds. Only a body above absolute zero (-273.15^oC) radiate energy to its surrounding. The electromagnetic radiation can vary widely.

2.3 TYPES OF THERMAL SOLAR COLLECTOR

A solar thermal energy collector is equipment in which solar energy is collected by absorbing radiation in an absorber and then transferring to a fluid. In general, there are two types of collectors:

2.3.1 Flat-Plate/Evacuated Tube Solar Collector

It has no optical concentrator. The collector area and the absorber area are numerically the same, the efficiency is low, and temperatures of the working fluid can be raised only up to 100°C.

Figure 2.1: Flat-plate collector

Source: Merriam-webster, (undated)

2.3.2 Concentrating-Type Solar Collector

The area receiving the solar radiation is several times greater than the absorber area and the efficiency is high. Mirrors and lenses are used to concentrate sun rays on the absorber, and the fluid temperature can be raised up to 500°C. For better performance, the collector is mounted on a tracking equipment to always face the sun with its changing position.

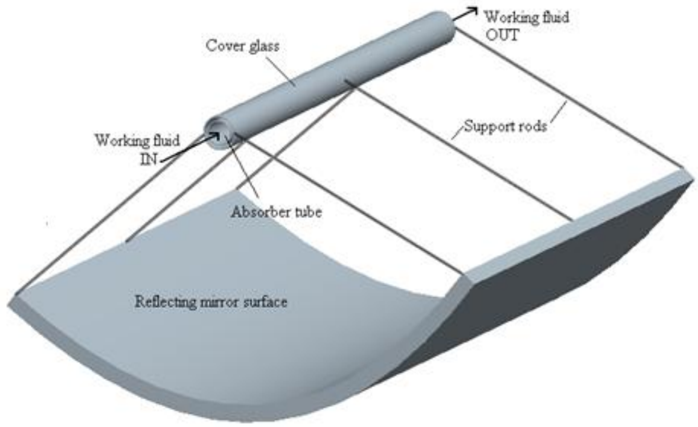

Figure 2.2: Concentrate collector

Source: New energy portal, (November 2009)

2.4 TECHNICAL ANALYSIS

SolidWorks simulation tools are software to verify the quality and performance of the design before it come to production. These comprehensive analysis tools let researchers design, analyze and simulate models, providing insight into the performance. The results can help to select or identify areas to reduce weight and often improve durability. Costs for development and material can be optimized to improve margins. The design alternatives can be compared to best meet specific requirements. Some of the analyses that will be used are:

2.4.1 Mechanism Design Analysis

Motion simulation provides quantitative information about the kinematic (position, velocity, and acceleration) and the dynamic (joint reactions, inertial forces, and power requirements) of all the components of a moving mechanism.

2.4.2 Stress Analysis

Linear stress analysis is routinely and accurately applied in the design phase of the projects. By setting up accurate fixtures, loading conditions, selecting the suitable mesh elements (beams, shell, or solid), and make skilled decisions on where to refine mesh for optimum results the detailed reports are produced by the software to help the researcher to understand the results. In this section, the strength-of-materials calculations (or analytical calculations) are performed to determine the effects of the design loads. The maximum-shear-stress theory is used to determine when these stresses will cause the hub to fail. The maximum-shear-stress theory predicts that if the three principal stresses are ordered $\sigma_1 > \sigma_2 > \sigma_3$, then yielding occurs when either the difference between σ_1 and σ_3 exceeds the material yield strength or the shear stress exceeds half of the material yield strength. The maximum-shear-stress theory was good for the design purposes because it is quick and easy to use. Furthermore, the maximum-shear-stress theory is a conservative predictor of failure. The shear stress and bending-moment stress are presented as bellow:

$$\text{Shear Stress, } \tau = \frac{\text{Shear Force}}{\text{Area}} = \frac{F_s}{A} \tag{2.1}$$

$$\text{Bending Stress} = \frac{Mc}{I} = \frac{M}{Section\ \ Modulus} \tag{2.2}$$

$$\text{Bearing Stress, } \sigma_b = \frac{Bearing\ \ Force}{Area} = \frac{F_b}{td} \tag{2.3}$$

Bearing stress obtained by dividing the load F_b by the area of the rectangle representing the projection of the bolt on the plate section. Since this area is equal to td, where t is the plate thickness and d is the diameter of the bolt.

2.4.3 The von Mises Stress

The distortion-energy theory (also called the shear-energy, von Mises Hencky, or octahedral-shear-stress theories) to determine when the design will fail. Detailed studies have indicated that yielding is related to the shear energy rather than the maximum shear stress. Strain energy is energy stored in the material due to elastic deformation. The energy of strain is similar to the energy stored in a spring. Upon close examination, the strain energy is seen to be of two kinds. One part results from changes in mutually perpendicular dimensions, and hence in volume, with no change angular changes. The other arises from angular distortion without volume change. The latter is termed as the shear strain energy, which has been shown to be a primary cause of elastic failure.

It can be shown by strain energy analysis that the shear strain energy associated with the principal stresses σ_1, σ_1 & σ_3 at elastic failure, is the same as than in the tensile test causing yield at direct stress σ' when:

$$\sigma' = \left[\frac{(\sigma_1-\sigma_2)^2 + (\sigma_2-\sigma_3)^2 + (\sigma_1-\sigma_3)^2}{2}\right]^{1/2} \tag{2.4}$$

In terms of simple linear stress combined with shear stress.

$$\text{Factor of Safety, } F.S = \frac{\sigma'}{{\sigma_x}^2 + (3{\tau_{xy}}^2)} \tag{2.5}$$

Failure will occur if $\sigma' \geq S_y$

The von Mises stress requires more computation than calculating the maximum shear stress, but it gives more realistic (less conservative) stress values than the maximum-shear-stress theory. Thus, the distortion-energy-theory is well suited to computational methods.

2.4.4 The Maximum Shear Stress Theory.

This is very relevant to ductile metals. It is conservative and relatively easy to apply. It assumes that failure occurs when a maximum shear stress attains a certain value and this value being the value of shear strength at a failure in tensile test. In this instance it is appropriate to choose the yield point as practical failure. If the yield point is S_y and this is obtained from a tensile test and thus is the sole principal stress then the maximum shear stress τ_{max} is easily identified as:

$$\tau_{max} = \frac{S_y}{2} \tag{2.6}$$

In the context of a complicated stress system the initial step would be to determine the principle stress σ_1, σ_1 & σ_3 in order of magnitude $\sigma_1 > \sigma_2 > \sigma_3$ then the maximum shear stress would be determined from the greatest of

$$\frac{\sigma_1 - \sigma_2}{2} = \frac{\sigma_1 - \sigma_3}{2}, \text{ or} \tag{2.7}$$

$$\frac{\sigma_2 - \sigma_3}{2} = \frac{\sigma_1 - \sigma_3}{2} \tag{2.8}$$

The factor of safety selected would be

$$F.S = \frac{S_y}{2\tau_{max}} = \frac{S_y}{\sigma_{1-}\,\sigma_3} \tag{2.9}$$

2.5 BUCKLING

When a slender member is subjected to an axial compressive load, it may fail by a condition called buckling**.** Buckling is not a failure of the material itself as is yielding and fracture, but is due to geometric instability of the system. Buckling is caused by a bifurcation in the solution to the equations of static equilibrium. At a certain stage under an increasing load, further load is able to be sustained in one of two states of equilibrium an undeformed state or a laterally-deformed state.

In practice, buckling is characterized by a sudden failure of a structural member subjected to high compressive stress, where the actual compressive stress at the point of failure is less than the ultimate compressive stresses that the material is capable of withstanding. For example, during earthquakes, reinforced concrete members may experience lateral deformation of the longitudinal reinforcing bars. This mode of failure is also described as failure due to elastic instability. Mathematical analysis of buckling makes use of an axial load eccentricity that introduces a moment, which does not form part of the primary forces to which the member is subjected. When load is constantly being applied on a member, such as column, it will ultimately become large enough to cause the member to become unstable. Further load will cause significant and somewhat unpredictable deformations, possibly leading to complete loss of load-carrying capacity. The member is said to have buckled, to have deformed.

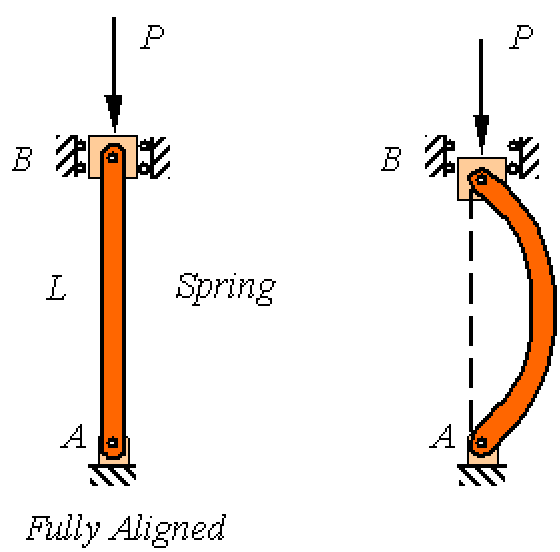

Figure 2.3: Buckling of columns

Source: Negahban, (1996)

2.5.1 Design Consideration

The ratio of the effective length of a column to the least radius of gyration of its cross section is called the slenderness ratio. This ratio affords a means of classifying columns. Slenderness ratio is important for design considerations. All the following are approximate values used for convenience.

Table 2.1: The short, intermediate and long classification of columns

Material	**Short Column** (Strength Limit)	**Intermediate Column** (Inelastic Stability Limit)	**Long Column** (Elastic Stability Limit)
	Slenderness Ratio ($SR = L_{eff} / r$)		
Structural Steel	$SR < 40$	$40 < SR < 150$	$SR > 150$
Aluminum Alloy AA 606-T6	$SR < 9.5$	$9.5 < SR < 66$	$SR > 66$
Aluminum Alloy AA 2014-T6	$SR < 12$	$12 < SR < 55$	$SR > 55$
Wood	$SR < 11$	$11 < SR < (18 \sim 30)$	$(18 \sim 30) < SR < 50$

Source: (Efunda, Undated)

In the Table 2.1, L_{eff} is the effective length of the column, and r is the radius of gyration of the cross-sectional area, defined as:

$$r = \sqrt{\frac{I}{A}} \tag{2.10}$$

A short steel column is one whose slenderness ratio does not exceed 50; an intermediate length steel column has a slenderness ratio ranging from about 50 to 200, and are dominated by the strength limit of the material, while a long steel column may be assumed to have a slenderness ratio greater than 200. A short concrete column is one having a ratio of unsupported length to least dimension of the cross section not greater than 10. If the ratio is greater than 10, it is a long column.

Timber columns may be classified as short columns if the ratio of the length to least dimension of the cross section is equal to or less than 10. The dividing line between intermediate and long timber columns cannot be readily evaluated. One way of defining the lower limit of long timber columns would be to set it as the smallest value of the ratio of length to least cross sectional area that would just exceed a certain constant *K* of the material. Since *K* depends on the modulus of elasticity and the allowable compressive stress parallel to the grain, it can be seen that this arbitrary limit would vary with the species of the timber. The value of *K* is given in most structural handbooks.

If the load on a column is applied through the center of gravity of its cross section, it is called an axial load. A load at any other point in the cross section is known as an eccentric load. A short column under the action of an axial load will fail by direct compression before it buckles, but a long column loaded in the same manner will fail by buckling (bending), the buckling effect being so large that the effect of the direct load may be neglected. The intermediate-length column will fail by a combination of direct compressive stress and bending.

2.6 STRESS CONCENTRATION

Stress concentration is defined as - Localized stress considerably higher than average (even in uniformly loaded cross sections of uniform thickness) due to abrupt changes in geometry or localized loading. Stress concentration is often called "stress raisers" or "stress risers". Geometric discontinuities cause localized stress increases above the average or far-field stress. A stress raiser's effect can be determined quantitatively in several ways, but not always readily. The simplest method, if applicable, is to use a known theoretical stress concentration factor, K_t, to calculate the maximum stress, σ_{max} from the nominal or average stress, σ_{ave}:

$$K_t = \frac{\sigma_{max}}{\sigma_{ave}} \tag{2.11}$$

The factor K_t depends mainly on the geometry of the notch, not on the material, except when the material deforms severely under load. K_t values are normally obtained from plots such as in Figure 2.5 and are strictly valid only for ideally elastic, stiff members. K_t values can also be determined by FEA or by several experimental techniques. There are no K_t values readily available for sharp notches and cracks, but one can always assume that such discontinuities produce the highest stress concentrations, sometimes factors of tens. This is the reason for brittle, high-strength materials being extremely sensitive even to minor scratches. In fatigue, for example, invisible tool marks may lead to premature, unexpected failures in strong steels.

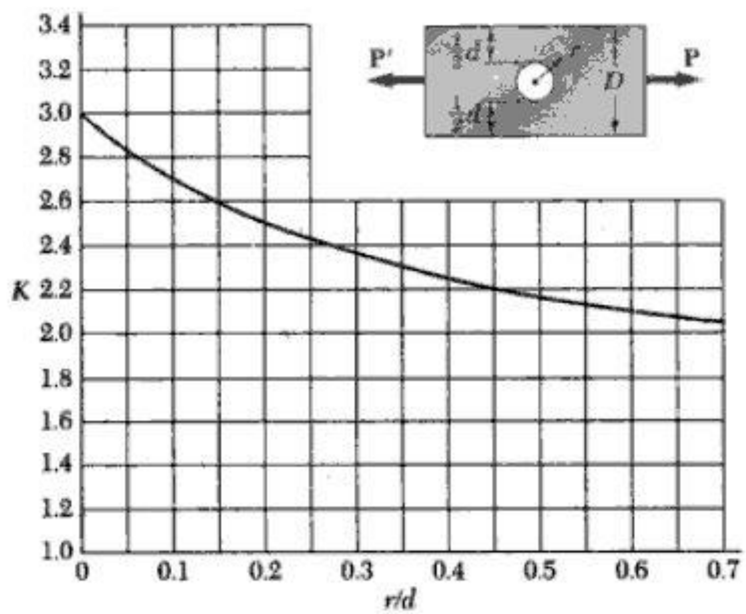

Figure 2.4: Stress concentration factor for flat bar with holes under axial loading

Source: Craig, R. R., Timothy A., (1934)

CHAPTER 3

METHODOLOGY

3.1 INTRODUCTION

Methodology can be defined as a sort of management and project planning from the beginning until the final stage of the project. The systematic planning of methodology is crucial to keep the project running smoothly. The designing and analysis process will be discussed in this chapter.

3.2 PROJECT FLOW CHART

A sequence of works has been planned carefully and is shown in figure 3.1. This project is divided into two sections, which are design and analyze.

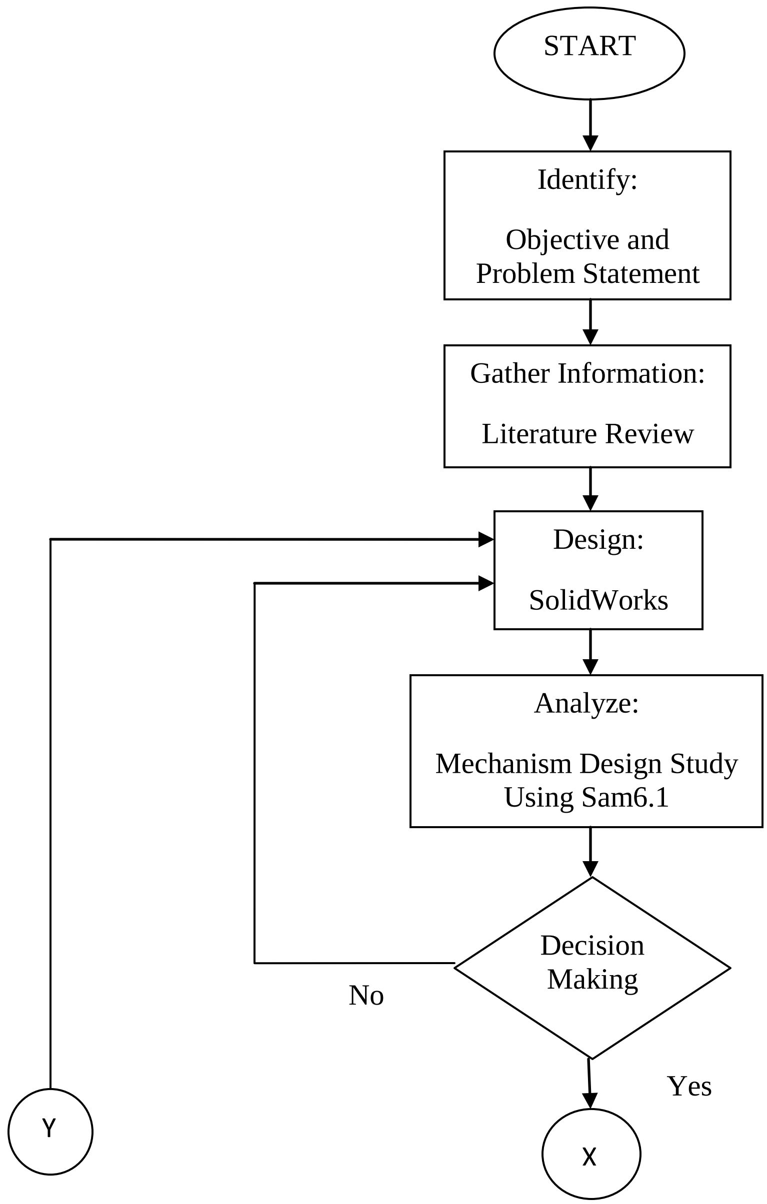

Figure 3.1: The methodology flow chart

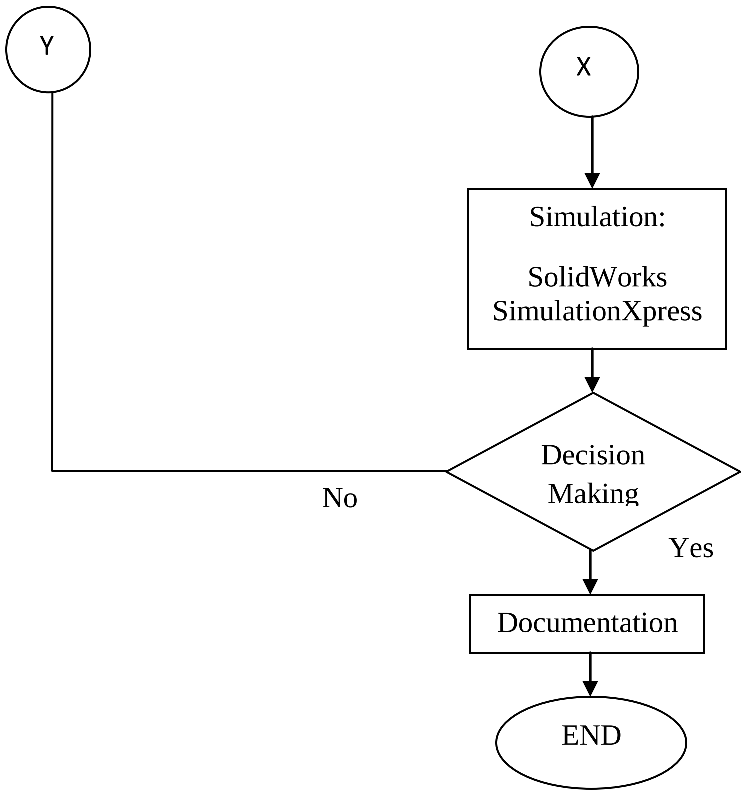

Figure 3.1: Continued

3.3 DESIGN

SolidWorks software was use in this study to design and analyze the model that was made. The design is using a full-scale of it actual size. The model is divided to five parts as shown in figure 3.10 to make it easier to draw and analyze. The divided parts are:

i. Frame
ii. Base
iii. Link
iv. Crank
v. Pin

3.3.1 Bill of Material

Table 3.1: Bill of material

Type	Size and thickness, mm	Length, mm	Quantity
Angles Bar	L50 x 50 x 3	600	1
		400	2
		1800	2
		1300	2
Flat Plate	50 x 6	120	6
		540	2
		800	2
	120 x 6	140	2
Hollow Bar	50 x 50 x 6	1700	1
		500	1
		1300	2

The designed part was design base on the material mentioned in table 3.1. The angle bar and flat plat was used in designing the frame. Flat plate was also used to design link and crank. The base is designed using hollow bar and stopper at the base part is designed using flat plate.

3.3.2 Material Selection

Stainless steel is the best material as it high ultimate strength 480-860 MPa, however due to limitation on the availability of the material, high density and high cost stainless steel is not economical to used as the main material for the study. Mild steel and aluminum had been identified as the next best choice of material. Aluminum has a low density but also low in ultimate strength. Thus mild steel as it moderate ultimate strength and density has been chosen and will be used to design the manual sun tracking system.

3.3.3 Frame

The frame was design to accumulate a 13000mm width and 1800mm length evacuated tube collectors. Seido 2-16 is used as the collector. The weight of the collector is 100kg as shown in table 3.3, thus the frame must be able to hold the collector in any angle. The size of the frame is exactly the same as the collector or an actual size of the collector. The material that was used in this study is steel (AISI 1020) with the mechanical properties as show in the Table 3.2.

The material used in this project is angles bar with the 50mm width and 3mm thick and flat bar with 100mm width and 6mm thick. This material was selected from other size and type of material from Faculty of Mechanical Engineering, University Malaysia Pahang store. The drawing of the frame is as Figure 3.2 and Figure 3.3.

Table 3.2: Mechanical Properties of the AISI 1020 steel

Property Name	**Elastic modulus, N/m^2**	**Poisson's ratio**	**Shear modulus, N/m^2**	**Mass density, kg/m^3**	**Tensile strength, N/m^2**	**Yield strength, N/m^2**
Value	2×10^{11}	0.29	7.7×10^{10}	7900	4.2051×10^{8}	3.5157×10^{8}

Source: A. K. Hosking and M. R. Harris. (Undated)

Table 3.3: Evacuated tube collectors 'Seido 2' Specification

Model	**Seido 2-8**	**Seido 2-16**
Design	Evacuated Tube with Flow-Through Design	Evacuated Tube with Flow-Through Design
Dimension (L×W×H), mm	2 126 x 960 150	2 126 x 1920 x 150
Number of tubes	8	16
Vacuum Tube Glass Material	high quality borosilicate	high quality borosilicate
Wall Thickness, mm	2.5	2.5
Tube Outside Diameter, mm	100	100
Tube Length, mm	2 000	2 000
Tube Weight, kg	4.55	
Hailstone Resistant to, mm	35	35
Collector Surface Area, m^2	2	4
Absorber Surface Area, m^2	1.4	2.8
Angle of Inclination, °	0-90	0-90
Module Weight, kg	50	100
Absorber Material	Aluminum	Aluminum
Selective Surface Coating	Aluminum Nitride	Aluminum Nitride
Absorption Coefficient	> 92%	> 92%
Emission Coefficient	< 8%	< 8%
Typical Operating Temperature, °C	70-120	70-120
Stagnation Temperature, °C:		
Module	190	190
Tube	276	276

Source: Alternative power distribution. (Undated)

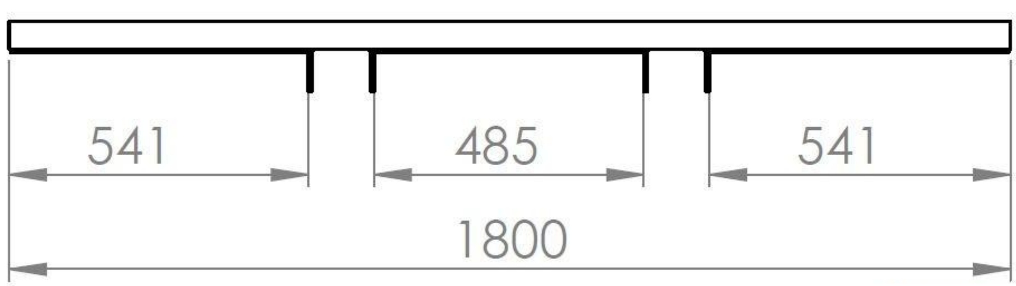

All dimensions in mm

Figure 3.2: The front view of the frame

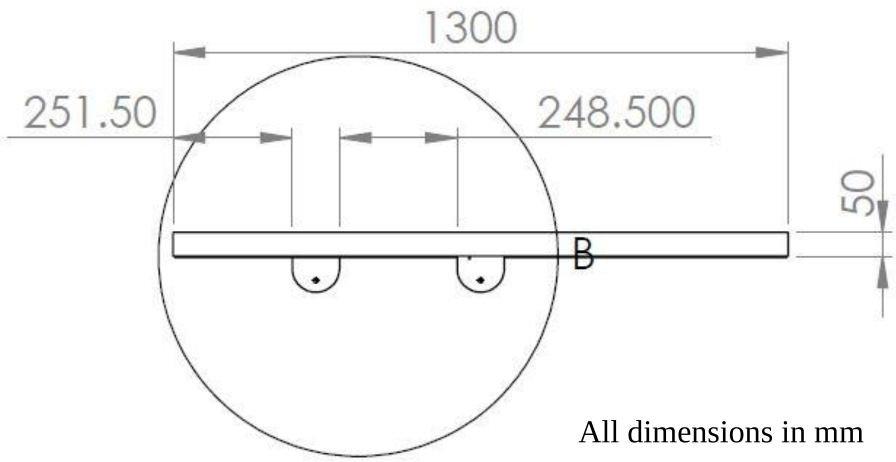

Figure 3.3: The right view of the frame

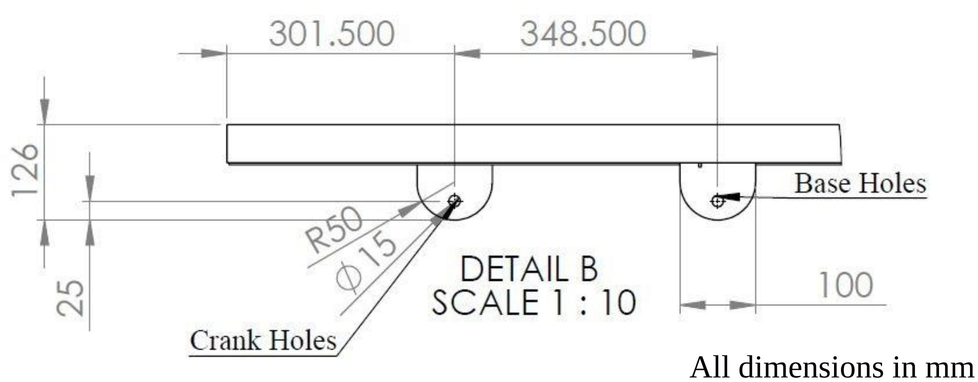

Figure 3.4: The close up view of the frame

The holes in the middle of the frame are named as base holes since the hole will be pinned to the base. The other holes are named as link hole which will be pinned to the link.

(Refer to Appendix B1)

3.3.4 Base

The base was design to hold the frame while the frame holds the solar collector. The base was design to allow the frame to rotate in one axis but with a limited angle. The material that was used to design the base is AISI 1020 steel with mechanical properties had been as in Table 3.2.

A hollow bar with 50mm width, 50mm length and 6mm thick and a flat bar with 50mm width and 6mm thick was used. The height of the base is 1350mm and the width is 1050mm while the length is 1600mm. The designed of the base part is as shown in Figure 3.5 and Figure 3.6.

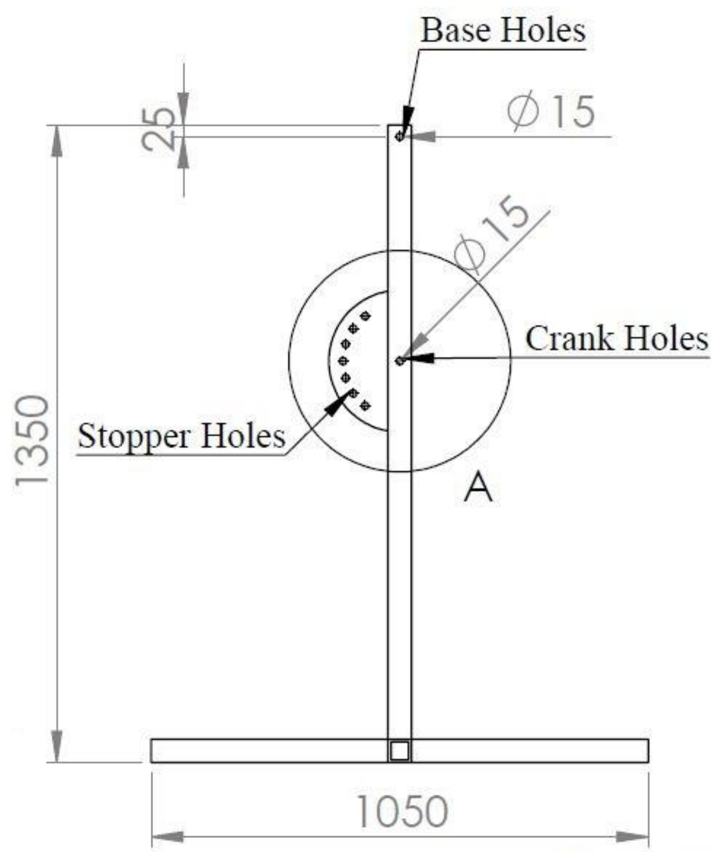

All dimensions in mm

Figure 3.5: The front view of the base

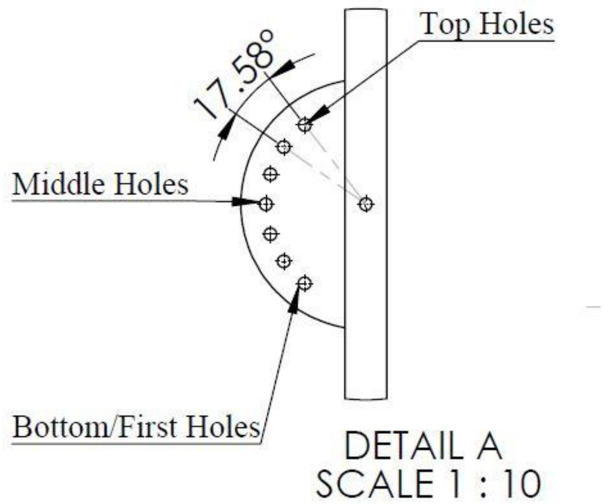

Figure 3.6: The close up right view of the base at the stopper

The half rounded shape in the middle of the base is designed to function as a stopper. The hole was made to allow the stopper pin installed there and the holes are named stopper hole. It also functions to distribute the load to the middle part of the base. The gaps between the holes are designed to a specific angle in order to let the frame be in a specific angle. The mechanism design study was made especially for this purpose. Each of the stopper holes are named with number so that it can be easily identified to simulate in the case study. The stopper hole from bottom is bottom hole or first hole. The middle hole is the holes at the middle of the stopper and at 180° from crank holes.

The other holes was named, the top holes at the base is named as frame holes since it will pined to the frame as shown in figure 3.5 and the holes in the middle part of the base is named as the crank holes because it will pined to the crank.

(Refer to Appendix B2)

3.3.5 Link

The link is design to transfer weight from frame to the middle part of the body. It was also used to transfer force and rotational movement that been applied to the crank. Flat bar with the width of 50mm and 6mm thick is used. The material that was used to design the link is AISI 1020 steel with mechanical properties as in Table 3.2.

This material was selected from other size and type of material from Faculty of Mechanical Engineering, University Malaysia Pahang store. The designed of the frame is as Figure 3.7.

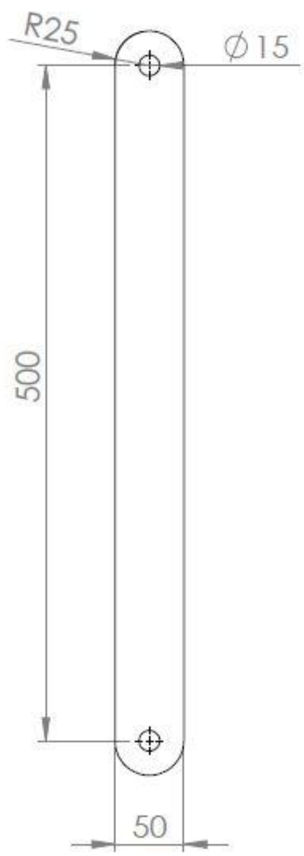

All dimensions in mm

Figure 3.7: The front view of the link

The height of the link is 540mm with two holes for fastening tool. The diameter of the holes is 15mm which is located 25mm from right, left, top and bottom side of the link. The gap between the holes is 500mm. The holes at the link is not named because it has the same dimension for both holes the only difference is that it located at the lower and upper side of the link.

(Refer to Appendix B3)

3.3.6 Crank

The crank is function to transfer the rotational force that been applied to the frame through link. By using a crank the frame can be rotated to the desired angle. Flat bar with the width of 50mm and 6mm thick is used. The material that was used to design the crank is AISI 1020 steel with mechanical properties as in Table 3.2.

This material was selected from other size and type of material from Faculty of Mechanical Engineering, University Malaysia Pahang store. The designed part of crank is as Figure 3.8.

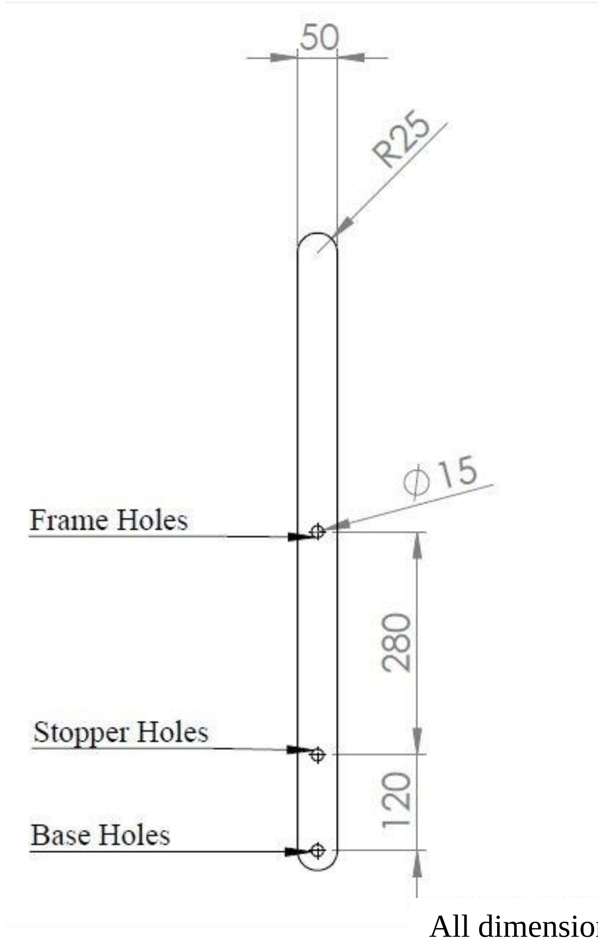

All dimensions in mm

Figure 3.8: The front view of the crank

The height of the crank is 8000mm with three holes which is two holes for the fastening tool while the other one is for stopper pin. The diameter of the holes is 5mm. The first hole is located 25mm from right, left and bottom side of the crank. The second and third hole was also located 25mm from right and left side of the crank but 130mm and 400mm from the first hole.

(Refer to Appendix B4)

3.3.7 Pin

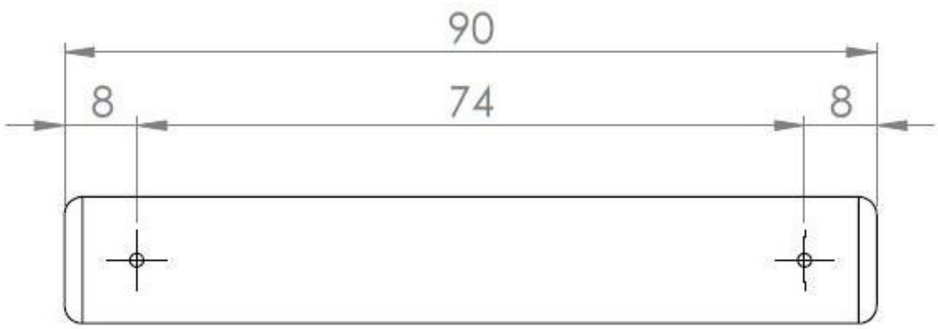

All dimensions in mm

Figure 3.9: The front view of the pin

The pin is function to secure the position of two difference part and allowed the part to move in an axis. Round bar with radius of 10mm is used. The material that was used to design the pin is AISI 1020 steel with mechanical properties as in Table 3.2.

This material was selected from other size and type of material from Faculty of Mechanical Engineering, University Malaysia Pahang store. The designed part of pin is as Figure 3.9.

(Refer to Appendix B5)

3.4 ASSEMBLY

After finish designing the four parts, the next step is assemblies which in this process, all of the part are assemble together to creating a whole new device. In this process, two links, two cranks, one base and one frame are used. The view of the assemblies is as Figure 3.10.

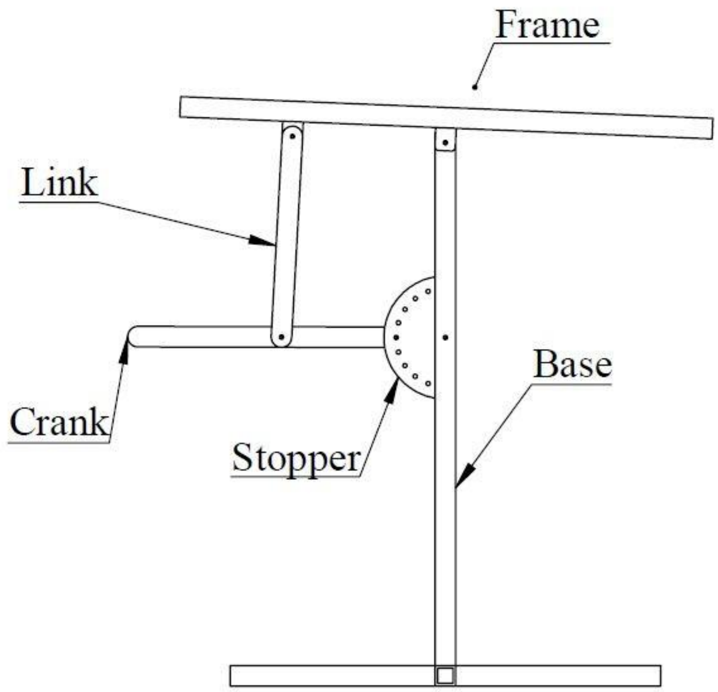

Figure 3.10: The front view of the assembly

The crank is assembling to the middle part of the base and stopper holes. The frame is assembly at the top of the base. The link is assembling between the crank and frame.

3.5 MESHING AND MODELING ASSUMPTIONS

The meshing process is the crucial parts in this study as it plays a major role in getting an accurate result and to verify the model. The setting for all parts is defined as the same in order to uniform the result except for the mesh condition. SolidWorks SimulationXpress is used to stimulate the design.

Table 3.3: Table of mesh information

	Mesh Information				
	Frame	**Base**	**Link**	**Crank**	**Pin**
Jacobian Check	4 Points	4 Points	4 Points	4 Points	4 Points
Element Size, mm	21.14	13.798	2.1499	3.088	1.31361
Tolerance, mm	1.057	0.6899	0.1075	0.1544	0.1154
Quality	High	High	High	High	High
Number of elements	20291	28970	56318	78204	18134
Number of nodes	40953	62633	95665	131872	47722

The design analysis results are based on linear static analysis and the material is assumed isotropic. Linear static analysis assumes that:

i. the material behavior is linear complying with Hooke's law
ii. Induced displacements are adequately small to ignore changes in stiffness due to loading
iii. Loads are applied slowly in order to ignore dynamic effects.

The following assumptions were necessary to reduce the model to a size that could mesh. The assumptions are:

i. The body is a full scale model from the original design.
ii. Symmetry boundary conditions are used in the modeling. The whole body is symmetric.

3.6 INPUT LOADS AND FIXTURE

3.6.1 Base

The load is calculated from the maximum stress located at the frame-base and frame-link holes gained from the finite elements analysis. The load is base on the average stress, σ_{ave} gain from calculation using stress concentration equation, equation 2.11. From σ_{ave}, then the bearing force, F_b is calculated using equation 2.3. The load was showed as the purple arrow in the Figure 3.11.

The loads were applied to the holes where the frame should be pinned to the base and a certain stopper holes. The study was divided to three case studies where it was to study the defect of the load applied to a different stopper holes. The first case study is the load is applied at the bottom stopper holes or the first holes from bottom of the stopper holes. The second case is at the middle part of the stopper holes or holes number five and the last case is the top stopper holes. The fix point is applied to the bottom part of the base since the base is located on the ground and should not be able to move. The fixture has been show as green arrow in the Figure 3.11.

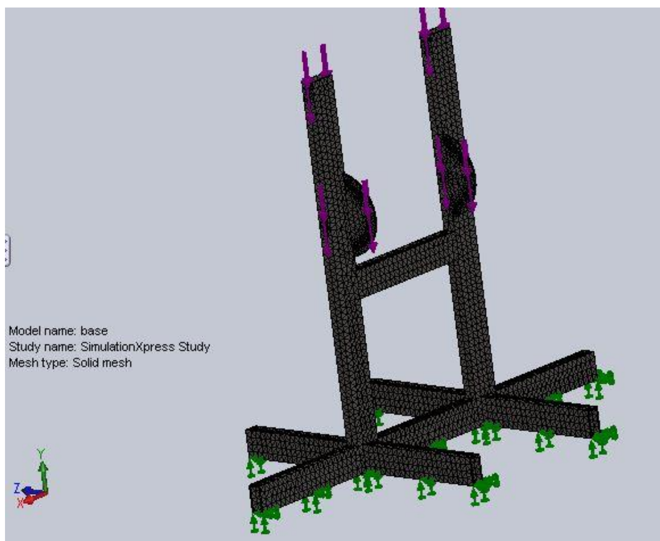

Figure 3.11: Mesh condition of the Base

3.6.2 Frame

The load is applied on the finite-element analysis model at the same location as the model that was build. The load is base on the weight of the solar collector that was used. The mass of the solar collector is 100 kg so the load that was applied to the frame is 1000 N which is the weight of the collector. Since the frame is design exactly the same size as the collector, so the load can be assumed to be uniform through the surface of the frame. The load was showed as the purple arrow in the Figure 3.12.

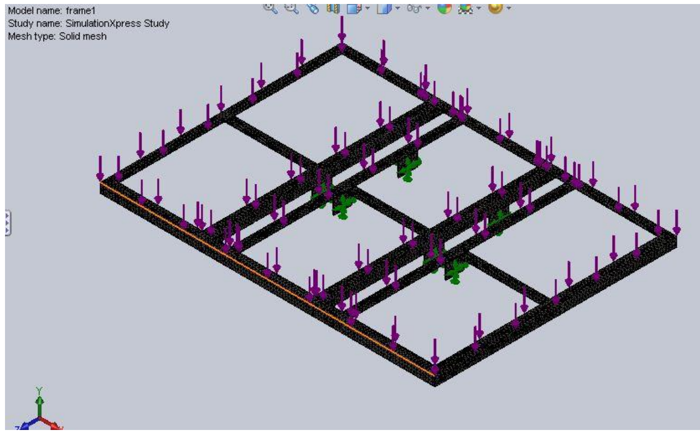

Figure 3.12: Mesh condition of the frame

There is no fix point at the drawing since all the holes in the design are pinned using fasteners but in this design study all the pinned hole are assumed as the fix point hence the fix point is applied in the simulation software. The fixture has been show as green arrow in the Figure 3.12.

3.6.3 Link

Figure 3.13: Mesh condition for the link

The load is applied on the finite-element analysis model at the same location as the model that was build. The load is base on the average stress, σ_{ave} gain from calculation using stress concentration equation, equation 2.11. From σ_{ave}, then the bearing force, F_b is calculated using equation 2.3. Since the link is design exactly the same size, so the load can be assumed to be uniform through the holes of the link. The load was showed as the purple arrow in the Figure 3.13. The load is applied at the top holes where the frame is connected and the fix point is at the bottom holes of the link where the crank is applied.

3.6.4 Crank

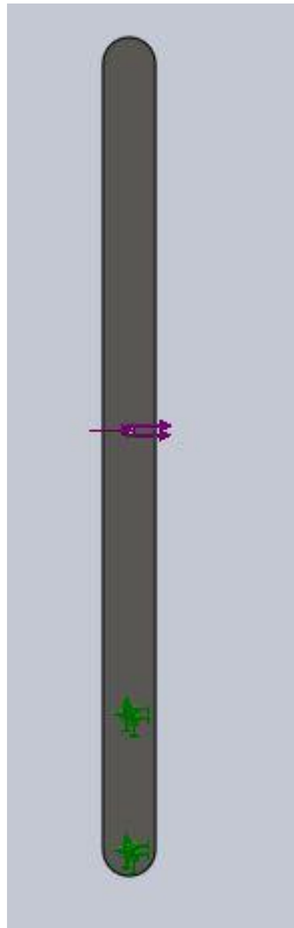

Figure 3.14: Mesh condition for the crank

The load is applied on the finite-element analysis model at the same location as the model that was build. The load is base on the average stress, σ_{ave} gain from calculation using stress concentration equation, equation 2.11. From σ_{ave}, then the bearing force, F_b is calculated using equation 2.3. Since the crank is design exactly the same size, so the load can be assumed to be uniform through the holes of the crank. The load was showed as the purple arrow in the Figure 3.14.The load is applied at the link holes where the link is connected and the fix point is at the stopper and base holes.

3.6.5 Pin

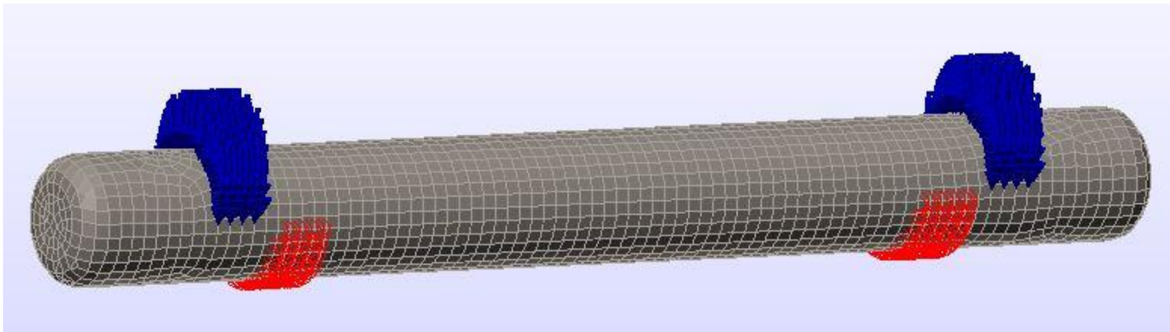

Figure 3.15: Mesh condition for the pin

The load is applied on the finite-element analysis model at the same location as the model that was build. The load is base on the average stress, σ_{ave} gain from calculation using stress concentration equation, equation 2.11. From σ_{ave}, then the bearing force, F_b is calculated using equation 2.3. Since the pin is design exactly the same size, so the load can be assumed to be uniform through the pin. The load was showed as the blue arrow in the Figure 3.15. The load is applied at the upper part where the pin is in contact with frame and the fix point is at the bellow part of the pin where the base is in contact with pin.

3.7 THE MECHANISM DESIGN STUDY

The mechanical design study was performed to study the movement of the designed mechanism. The study was done using Sam6.1 software. A two dimensional study was performed since the design can only rotate in one axis only. The frame is define as link 3, the link as link 4, the crank as link 1 and the base are define as fix point since the base are designed not to move. The study is defined as one degree of freedom since it can only move in one rotational axis. The study was done as in the Figure 3.16. The frame has been defined as the source of the motion. The study was done at 180° of the crank. The crank than rotated for 20° to get the rotational angle of the frame. The maximum displacement of the frame also will be determined in this study.

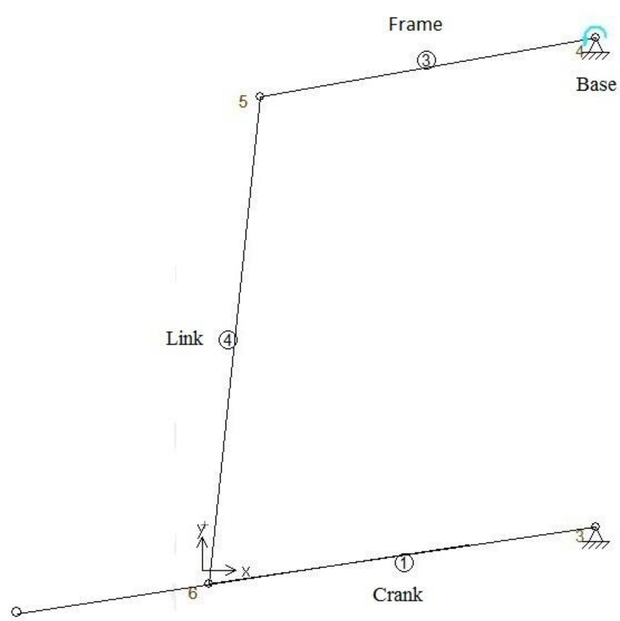

Figure 3.16: The mechanism design study

CHAPTER 4

RESULT AND DISCUSSION

4.1 INTRODUCTION

This chapter of study is made to show and discuss of the result that been gained from the simulation that been made. In this chapter the result will be discuss so that the modification or future work planning can be made. In the previous chapter a few simulation has been design such as finite element analysis (FEA) using SolidWorks SimulationXpress, Algor(FEMPRO) and Mechanism Design Study using Sam6.1.

The objectives for SolidWorks SimulationXpress and ALGOR FemPro is to study the stress, safety factor and the deformation of the design while mechanism study using SAM6.1 is to study the movement of the designed mechanism.

4.2 LOAD AND STRESS CALCULATION

Table 4.1: Data for load and stress calculation at the holes

Holes Positon	σ_{max}, **N/mm^2**	K_t	σ_{ave}, **N/mm^2**	F_b, **N**
Base holes at frame	44.563	2.49	17.92	1 612.8
Link holes at frame	35.654	2.49	14.32	1288.8
Crank holes at link	18.259	2.49	7.32	658.92
Stopper holes at crank	22.715	2.49	9.12	820.8
Base holes at crank	11.357	2.49	4.56	410.49

The maximum stress at the holes is obtained from the FEA analysis as shown in table 4.1. The maximum stress value is than be assumed base on the color at the holes. For an example calculation for base holes at frame, let σ_{max} = 44.563 N/mm^2
The K_t value is taken from figure 2.5 after r/d is calculated.

$$r/d = \frac{7.5}{35} = 0.125$$

From figure 2.4, K_t = 2.49. Then the σ_{ave} is calculated using equation 2.11.

$$K_t = \frac{\sigma_{max}}{\sigma_{ave}}$$

$$\sigma_{ave} = \frac{\sigma_{max}}{K_t} = \frac{44.563}{2.49} = 17.92 \text{ N/mm}^2$$

Then the bearing force, F_b is calculated from equation 2.3. The σ_{ave} is assumed to equal the σ_b.

$$\sigma_b = \frac{F_b}{td}$$

Bearing force for base holes at frame, F_b

$$F_b = \sigma_b \times td = 17.92 \times (6 \times 15) = 1\,612.8 \text{ N}$$

The F_b value is used to applied load to the pin and frame holes at base.

Each F_b was applied to different place where $F_{b,\ link\ @\ frame}$ is used as load on frame holes at link. $F_{b,\ crank\ @\ link}$ is used as load on link holes at crank. $F_{b,\ stopper\ @\ crank}$ is used as load on stopper holes at base. $F_{b,\ base\ @\ crank}$ is used as load on crank holes at base.

4.3 FINITE ELEMENT ANALYSIS

This analysis has been done to every parts of the design which is frame, pins, crank, link and base.

4.3.1 Frame

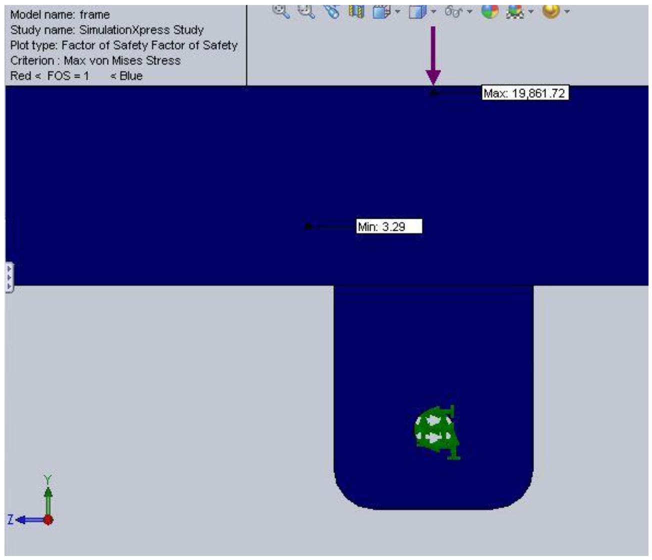

Figure 4.1: Safety factors for frame at base holes

Figure 4.1 shows the safety of the frame that was designed using mild steel. It shows that all part of the frame is having a safety factor higher than one which means that this designed frame are applicable to be used as the frame that can hold the solar collector. The lowest safety factor for this designed frame is 3.29 which are higher than one but it is not very high so no optimization of the part is needed.

The outer part of the frame are recommended to be optimize because of the safety factor value is very high. It is recommended that the outer part of the frame is to design using different type of the material or smaller size of mild steel bar. The different value of the safety factor for frame between the outer part and the center of the frame where the holes connected the frame with the base is because of the stress concentration are concentrated to the center of the frame thus the lowest safety value should be on the base holes but it did not happen in this analysis. Instead it happens at the eagle bar that is close to the flat bar that where the base holes are. It is because of the stress concentration is toward the center and bending moment that the eagle bar experience.

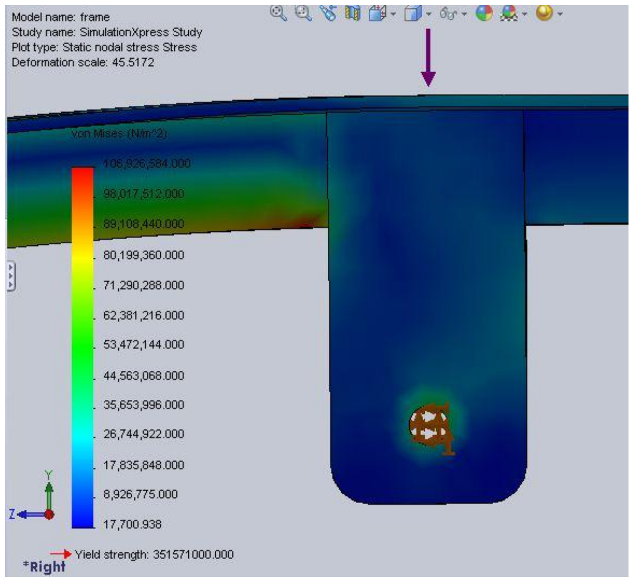

Figure 4.2: von Mises stress at base holes for frame

Figure 4.2 show the von Mises stress for the frame. The maximum von Mises stress for the frame is 106.927 N/mm^2 (MPa) at the same position of the minimum safety factor value and so do the minimum stress is at the maximum safety factor value with the stress value of 0.018 N/mm^2 (MPa). It is occur that the stress value is inversely proportional to the safety factor value. The safety factor value is calculated by dividing the ultimate stress with the allowable stress. The ultimate stress is the maximum stress value that the material can stand and the allowable stress is the stress that is experience by the designed frame by applying force.

The total maximum of displacement of this designed frame is 3.96mm. This displacement is because of the bending moment that the frame experience. The solar panel that was used to collect the solar radiance are not allowed to bend because it will break the solar panel, however the frame will take time to bend so it will give a useable life time to the frame. It is mean that the frame can be used for a period of time. The life time of the frame before it bend are unknown thus further study and field test are required to determine the time taken for the frame to bend and the effect of the displacement to the solar panel. To avoid the frame to have any displacement, modification is needed. A bigger width eagle bar and flat bar are better at withstanding the bending moment.

4.3.2 Link

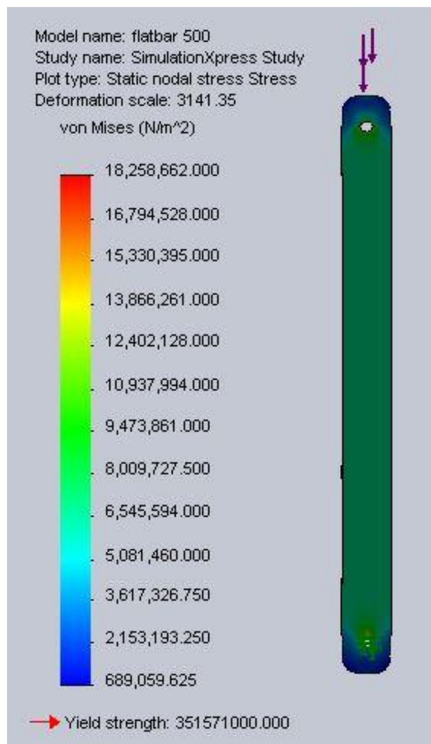

Figure 4.3: von Mises stress for link

Figure 4.3 show the von Mises stress for the link. The maximum von Mises stress for the link is 18.2587 N/mm^2 (MPa) at the upper hole of link. The minimum stress is at the bottom of the link with the stress value of 0.6891 N/mm^2 (MPa). The result shows that the stress concentration is higher nearing the holes.

The total maximum of displacement of this designed link is 0.0017 mm. the maximum displacement of the link is very low thus it will not affect the performance of the mechanism. The designed link also did not buckle under given loading thus it showed that the link was properly designed and stable.

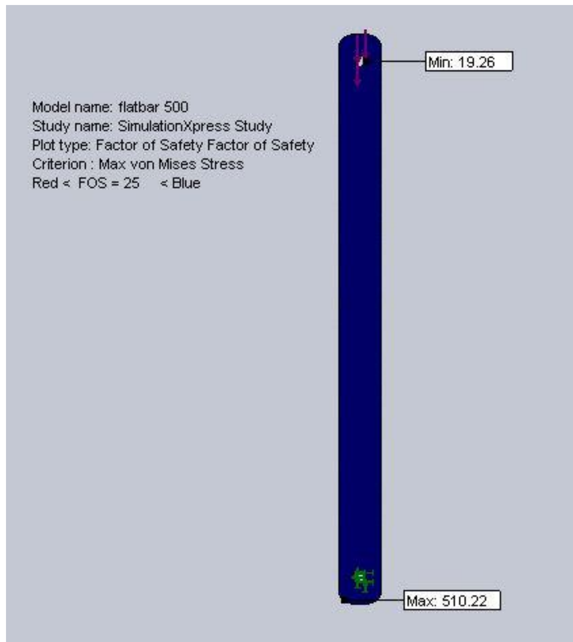

Figure 4.4: Safety factors for link

Figure 4.4 shows the safety of the link that was designed using mild steel. It shows that all part of the link is having a safety factor higher than one which means that this designed link is applicable to be used. The lowest safety factor for this designed link is 19.26 which are higher than one and no optimization of the part or modification is needed. It shows that the link is properly designed and any change in design may cause unstable stress distribution across the link and buckling may occur.

4.3.3 Crank

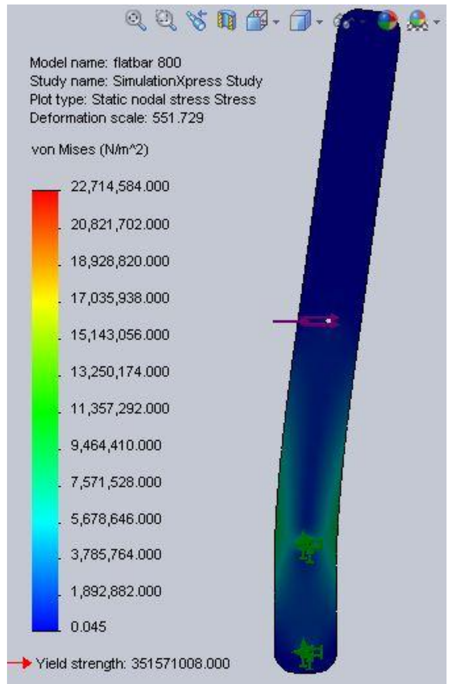

Figure 4.5: von Mises stress for crank

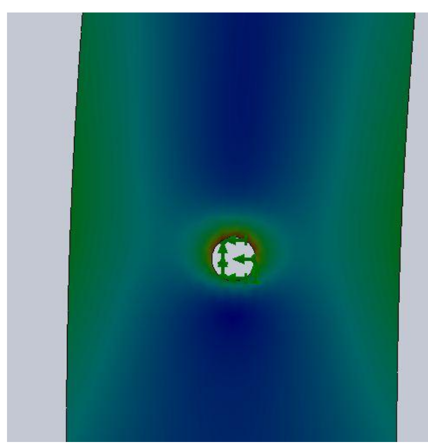

Figure 4.6: Close up view of von Mises stress at stopper holes

Figure 4.5 and figure 4.6 show the static nodal stress for the crank. The maximum von Mises stress for the crank is 22.7146 N/mm^2 (MPa) at the stopper holes of crank. The minimum stress is at the both end of the crankk with the stress value of 4.54×10^{-2} N/mm^2 (MPa). The result shows that the stress concentration is highest at the holes and high at the edge of the crank near the stopper holes.

The total maximum of displacement of this designed crank is 0.145 mm. The maximum displacement of the crank is very low thus it will not affect the performance of the mechanism. The designed crank did bend under given loading but it still under effective length thus the crank was properly designed and stable.

The lowest safety factor for this designed crank is 15.48 which are higher than one there is no need for modification and optimization to the crank because the crank is properly designed and any change in design may cause unstable stress distribution across the crank and buckling may occur.

4.3.4 Pin

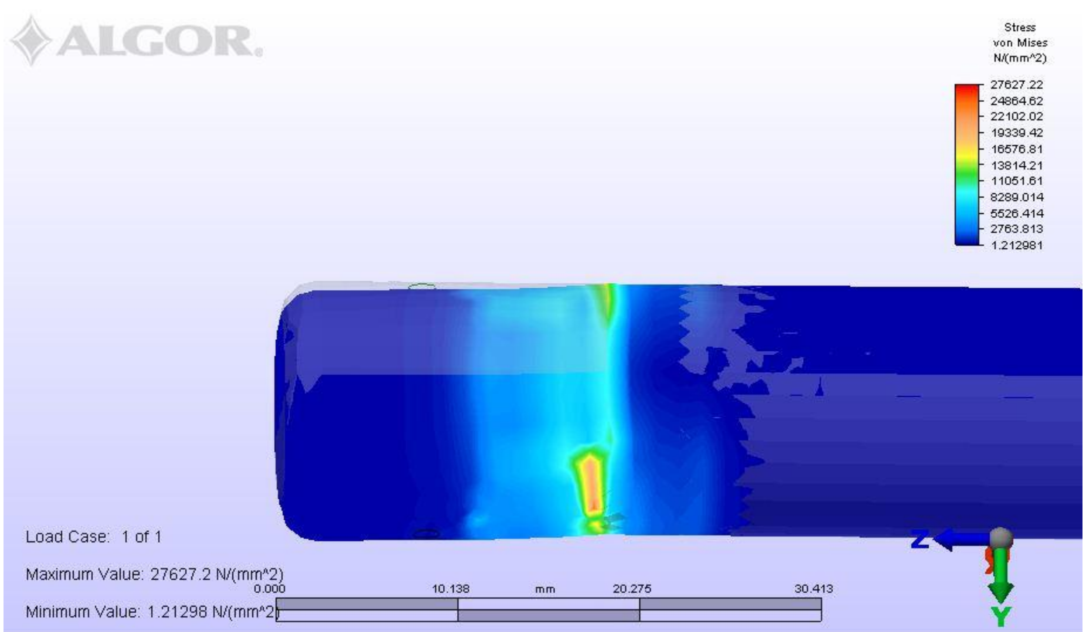

Figure 4.7: von Mises Stress for frame – base pin

Figure 4.7 shows the stress that the frame – base pin experiencing. The pin is experiencing double sheer stress with the maximum von Mises stress value is 27.63 N/mm^2 and the minimum von Mises stress value is 0.012 N/mm^2. The maximum stress occurs in between base hole and frame holes. It is because of the sheering stress are concentrate at the cross sectional area of the pin.

The maximum displacement for this pin is 0.069mm which is very low and can be neglect as it no means since the holes are design with 1mm tolerance.

4.3.5 Base

The designed base part is experiencing deformation with the deformation ratio of 11 728.8. The deformed design is shown in Figure 4.8

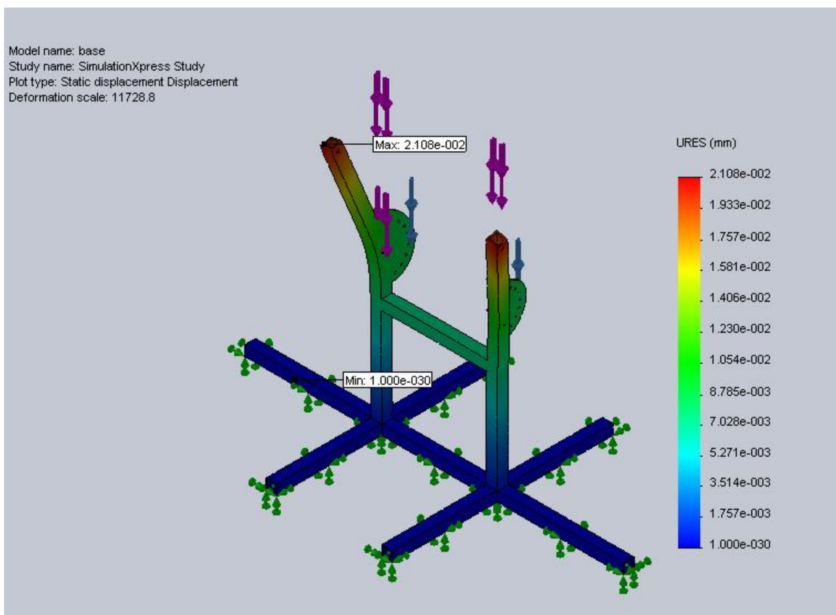

Figure 4.8: Static displacement for base

Figure 4.8 show the static displacement for base. It shows that the maximum displacement is on top of the base design and the lowest displacement is at the bottom of the design and it goes the same for the other case. The maximum value of displacement is the same as for all cases which 0.02108 mm.

For the von Mises stress, the stress is high at the pined holes, stopper part and bellow of the crank holes depends on the case study. The minimum value of stress is at the bottom of the base but the maximum value is depends on the cases study. The minimum stress value is 4.542×10^{-7} N/mm^2 (MPa) and the maximum value is 7.455 N/mm^2 (MPa) located at stopper holes. Figure 4.9 show the stress distribution on the base.

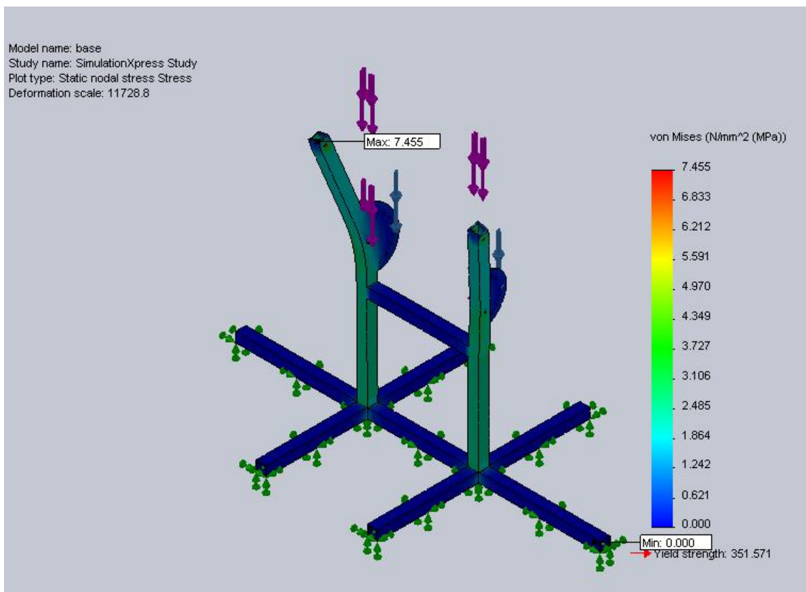

Figure 4.9: von Mises stress for base case 2

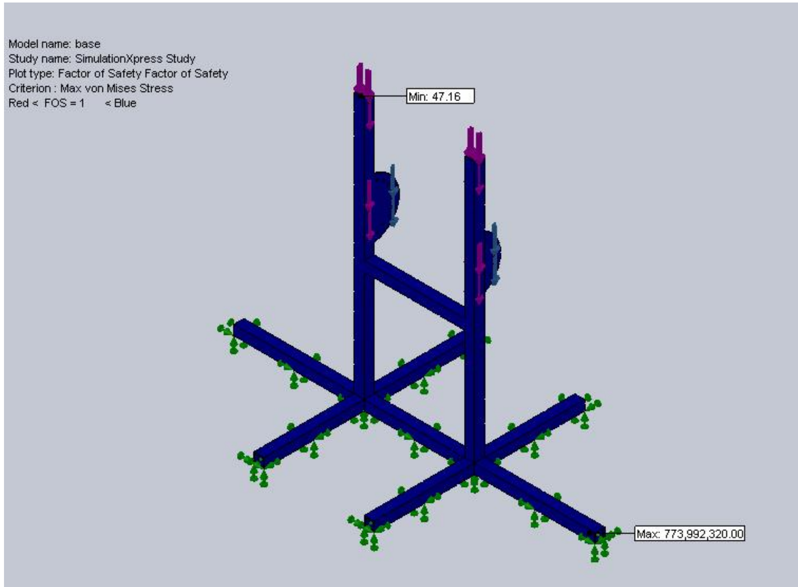

Figure 4.10: Safety factors for base

Figure 4.10 show the safety factor for the base case two. As show in the figure 4.10 the safety factor that bigger than one is show in blue color while less than 1 is show in red. Every hole that was applied load is having safety factor bigger than one while other parts also are having various safety factor. The faces that align with stopper and position bellow the stopper and crank holes are having safety factor bigger than one where the stress value are high. The minimum value of the safety factor is 47.16 on the top of the base where the frame hole is.

The designed base part is properly designed. It has a very low value of displacement thus it show that the base did buckle but still in allowable scale. The lowest safety factor for the base is very high. Thus it shows that the base is very safe design.

4.4 MECHANISM DESIGN STUDY

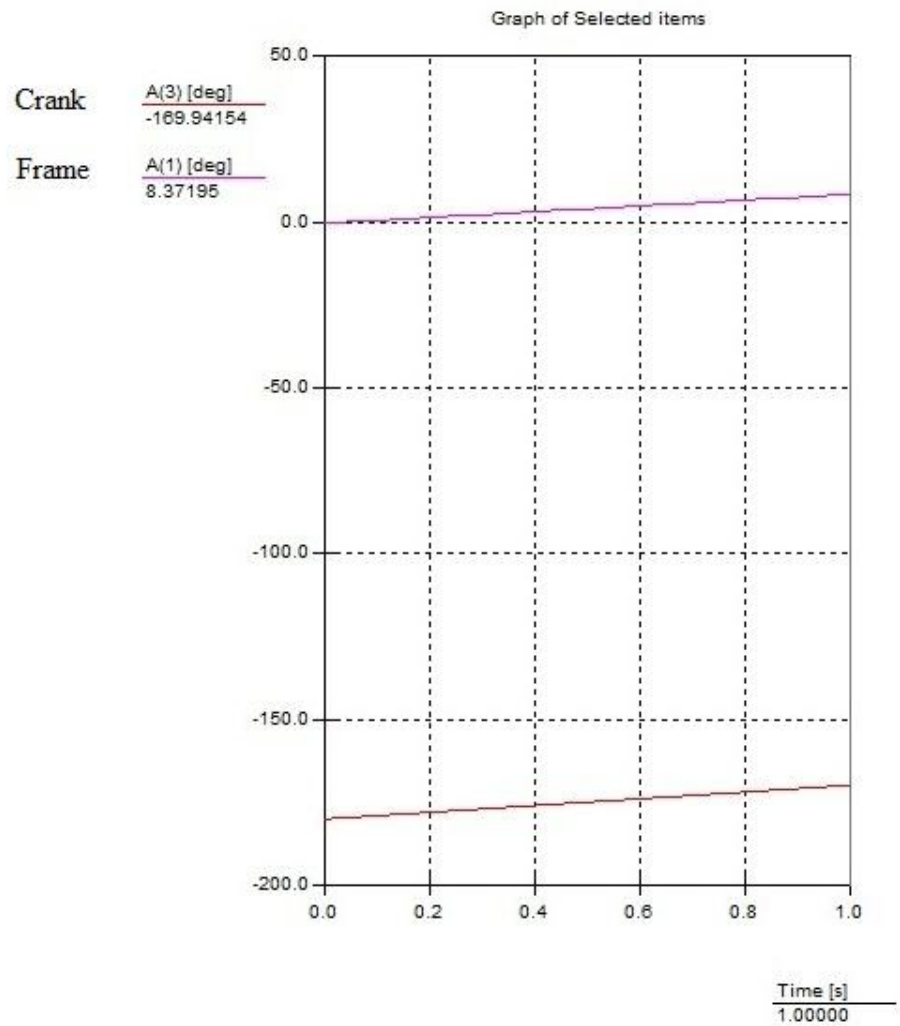

Figure 4.11: Graph of displacement of the frame and crank

Figure 4.11 show the mechanism movement when the crank is rotated. The crank rotates at 8.702° cause the frame to rotate 10°. The designed manual sun tracking system is aiming as 20° as the angle different for each stop in order to allow the solar collector to absorb solar radiation at certain angle. For the frame to rotate in 20°, the crank must rotate to 17.404°. The stopper holes are designed base on this study. The gaps of each stopper holes are 17.404° so that the frame will have 20° difference in each stopper holes.

CHAPTER 5

CONCLUSIONS AND RECOMENDATION

5.1 CONCLUSION

Although the design has not yet being prototyped and tested but it should satisfy all the design specifications. The analysis shows that the designed part can hold the load that applied to it. All part of the designed part is having more than 1 value of the safety factor.

The time taken to finish this study is longer than it should but by using SolidWorks software to design and analyze really help to reduce the time taken. The experimental data and practical experience are to be used in conjunction with this data. Field testing is mandatory to validate the final design. This study is to help to reduce time time-to-market by reducing but not eliminating field tests.

The mechanism design study using Sam6.1 really help to understand how the design work which in this study when the crank is rotate to 17.404° the frame will rotate to 20°. It shows that the manual sun tracking system can follow the sun position as it primary function. The SolidWorks software also have the capability to performed this analysis which it can give more clear data and view of the result since it can simulate a three dimensional design where Sam6.1 can only simulate in two dimensional.

5.2 RECOMMENDATION

For further studies of this project, the recommendations have been identified as follows:

i. The other simulation software such as ALGOR(FEMPRO) or CATIA can be used to simulate the design to give more variable data so that a comparison can be made.
ii. Pin design is recommended to use a bigger diameter to get more surface area. It is also recommended to design the pin to take double or multiple sheer stress rather than single sheer.
iii. Developing prototype is a very crucial step should be taken after this study because only by doing so the field test can be done. Furthermore the effect of the solar tracking system can also be tested.
iv. It is also be better if the sun tracking system has its own automatic moving system such as Programmed Logic Circuit (PLC), MicroP or MicroC.
v. Using hydraulic or motor to move the mechanism are also recommended to make the sun tracking system user friendly.

REFERENCE

A. K. Hosking and M. R. Harris. *Mechanical Design*. Seconded Ed. USA: H & H Publishing. p1.26.

Alternative power distribution. Undated. Online Source. Criteria: Seido 2 specification. http://alternativepowerdistribution.com/seido-2-specs.html

Beer, F. P., Johnston, E. R. Jr. and Dewolf, J. T. 2006 *Mechanics of Materials.* Fourth ed. Singapore: McGraw-Hill

Benham, P. P., Crawford, R.J., and Armstrong, C. G. 1996 *Mechanics of Engineering Materials*. Pearson Education Limited

Budynas, R. G., Nisbett, J. K. "Shigley's Mechanical Engineering Design"

Cotrell, J. June 2002. The Mechanical Design, Analysis, and Testing of a Two-Bladed Wind Turbine Hub. NREL/TP-500-26645

Craig, R. R. and Timothy A. 1934 *Mechanics of Materials.* Third ed. USA: John Wiley and Sons, Inc.

Efunda. Undated. Online Source. Criteria: Classification of columns. http://www.efunda.com/formulae/solid_mechanics/columns/intro.cfm

German Advisory Council on Global Change. 2003. Online source. Criteria: Global change. http://www.wbgu.de

João M. G. Figueredo, José M. G. Sá da Costa "Intelligent Sun-Tracking System for Efficiency Maximization of Photovoltaic Energy Production".

Khan, N., Mariun, Z. and Saleem, N. 2007 . Fossil Fuels, New Energy Sources and the Great Energy Crisis. Renewable and Sustainable Energy Rev (2007)

Meriam-webster. Undated. Online source. Criteria: Flat-plate solar collector. http://visual.merriam-webster.com/energy/solar-energy/flat-plate-solar-collector_2.php

Negahban, ã. M. 1996-2000. Online Source. Criteria: Buckling of columns. http://emweb.unl.edu/NEGAHBAN/Em325/21-Buckling%20of%20columns/Buckling%20of%20columns.htm

New energy portal. November 2009. Online source. Criteria: Concentrate collector. http://newenergyportal.wordpress.com/2009/11/26/parabolic-trough-collector-system/

Raghavan, V. 2001. *Material Science and Engineering*. New Delhi: Prentice-Hall edition of India, Inc.

APPENDIX A1

GANTT CHART FOR FYP 1

Project Activities	W1	W2	W3	W4	W5	W6	W7	W8	W9	W 10	W 11	W 12	W 13	W 14
Literaure Review	■	■	■	■	■	■	■	■	■	■	■			
Project Understanding	■	■	■	■	■	■								
Objective and Scopes			■	■	■	■								
Methodology			■	■	■	■	■	■	■	■	■			
Expected Result									■	■	■	■	■	
Presentation Preparation												■	■	
Presentation														■

APPENDIX A2

GANTT CHART FOR FYP 2

Project Activities	W1	W2	W3	W4	W5	W6	W7	W8	W9	W 10	W 11	W 12	W 13	W 14
Design using SolidWorks														
Simulation														
Mechanism Analysis														
Compare Result														
Making Conclusion														
Report Preparation														
Presentation														

APPENDIX B1

DRAWING OF THE FRAME

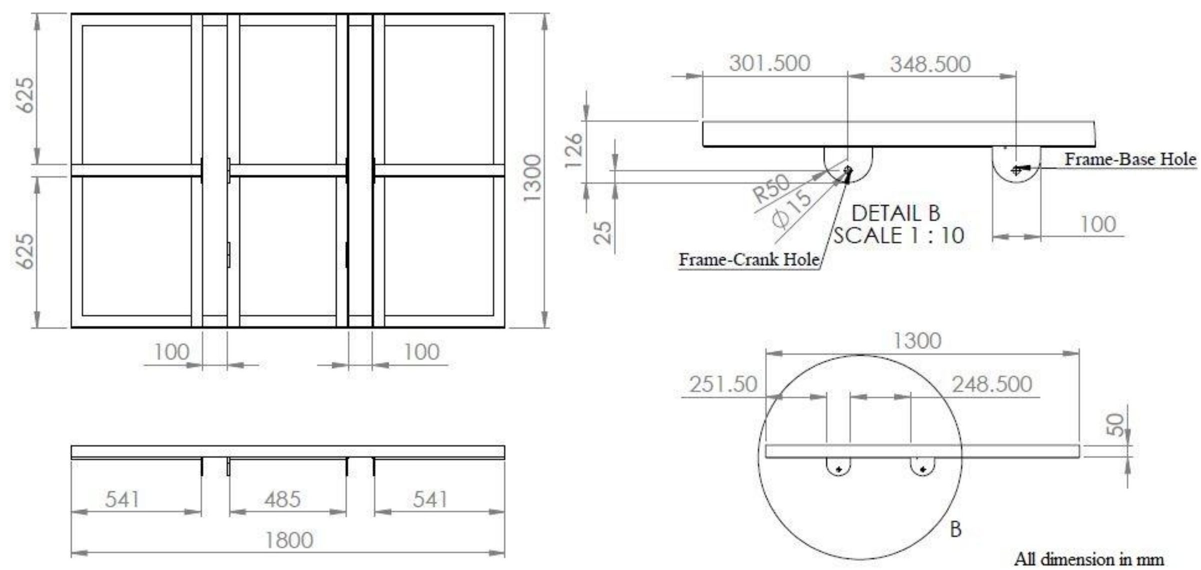

Figure 6.1: Two- dimensional drawing of frame

APPENDIX B2

DRAWING OF THE BASE

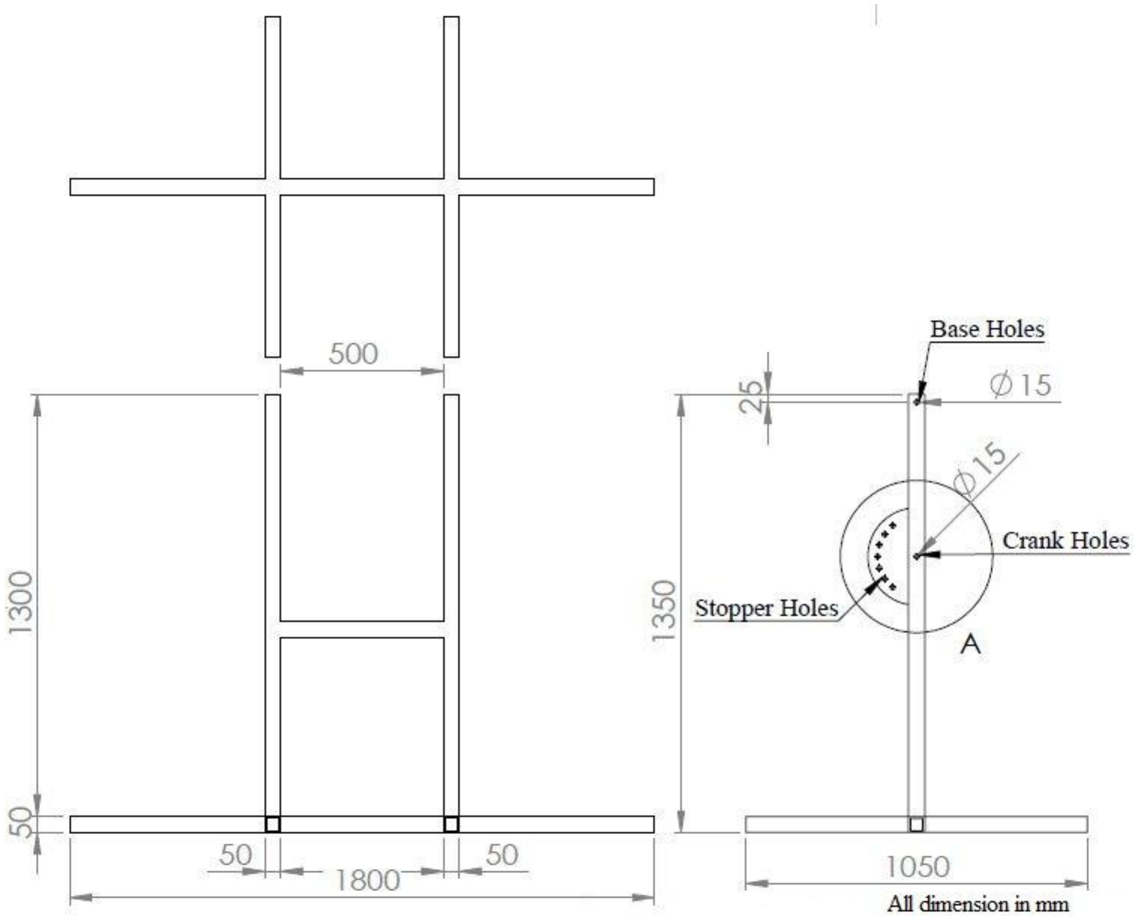

Figure 6.2: Two- dimensional drawing of base

APPENDIX B3

DRAWING OF THE LINK

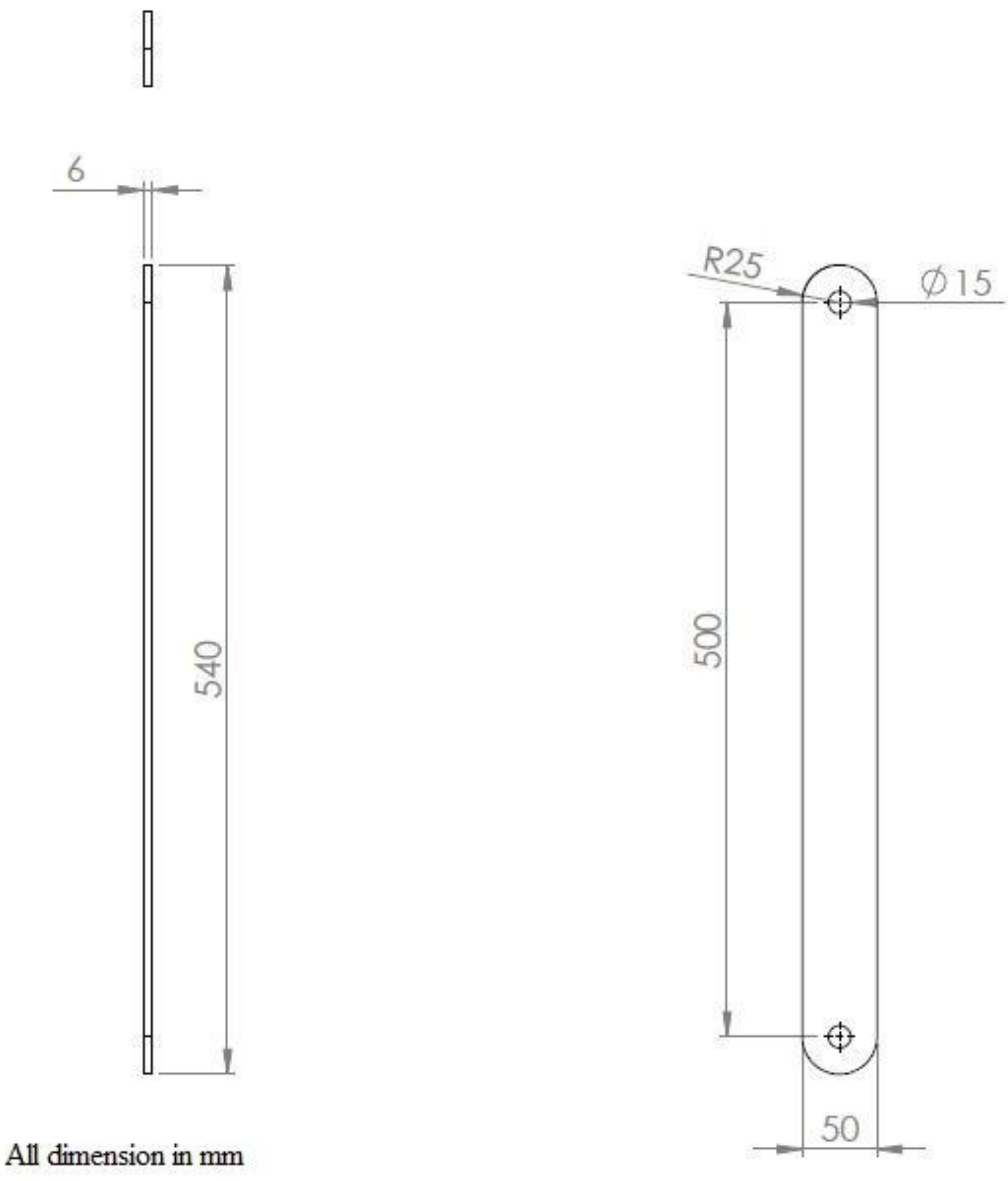

Figure 6.3: Two-dimensional drawing of the link

APPENDIX B4

DRAWING OF THE CRANK

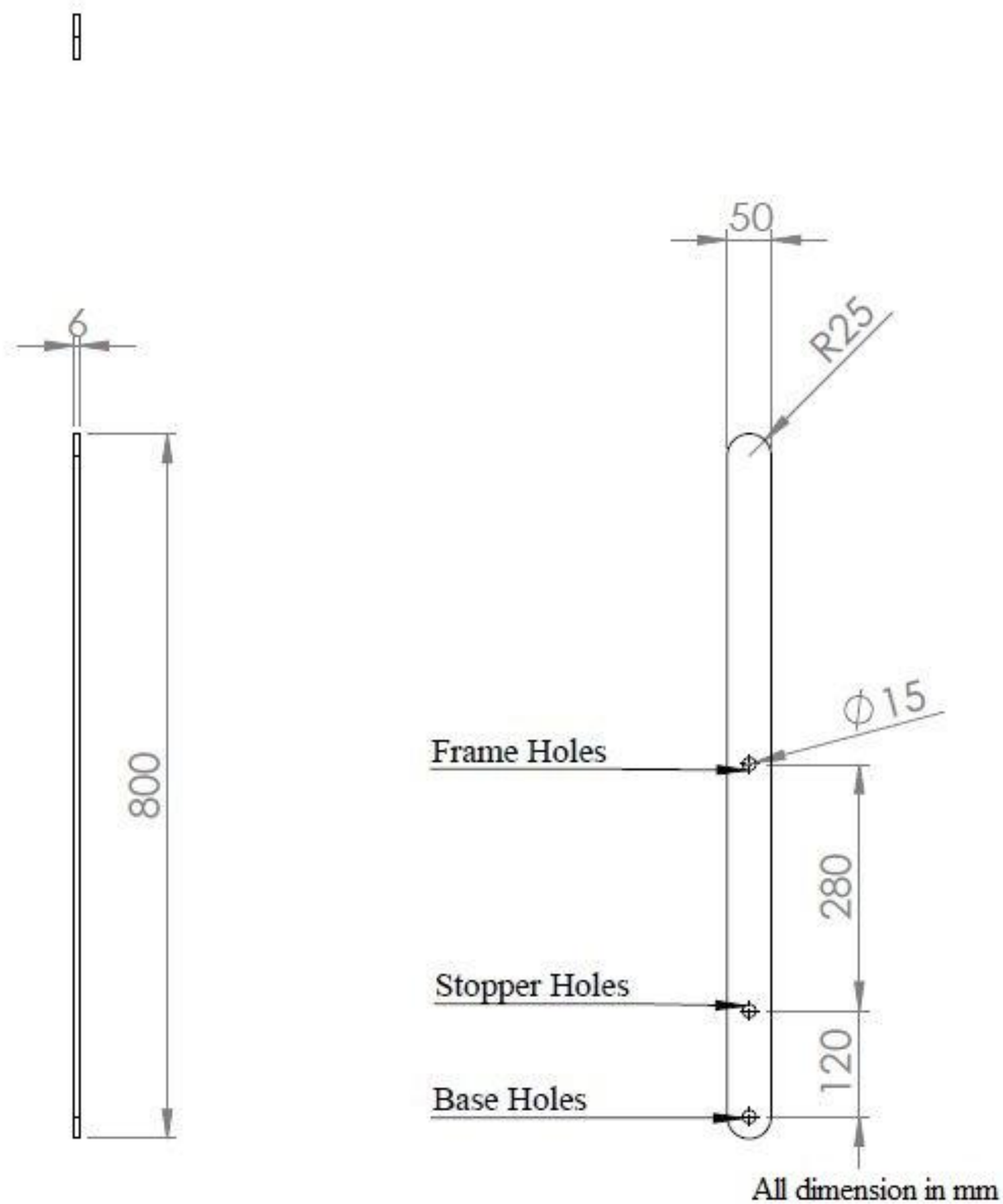

Figure 6.4: Two-dimensional drawing of the crank

APPENDIX B5

DRAWING OF THE PIN

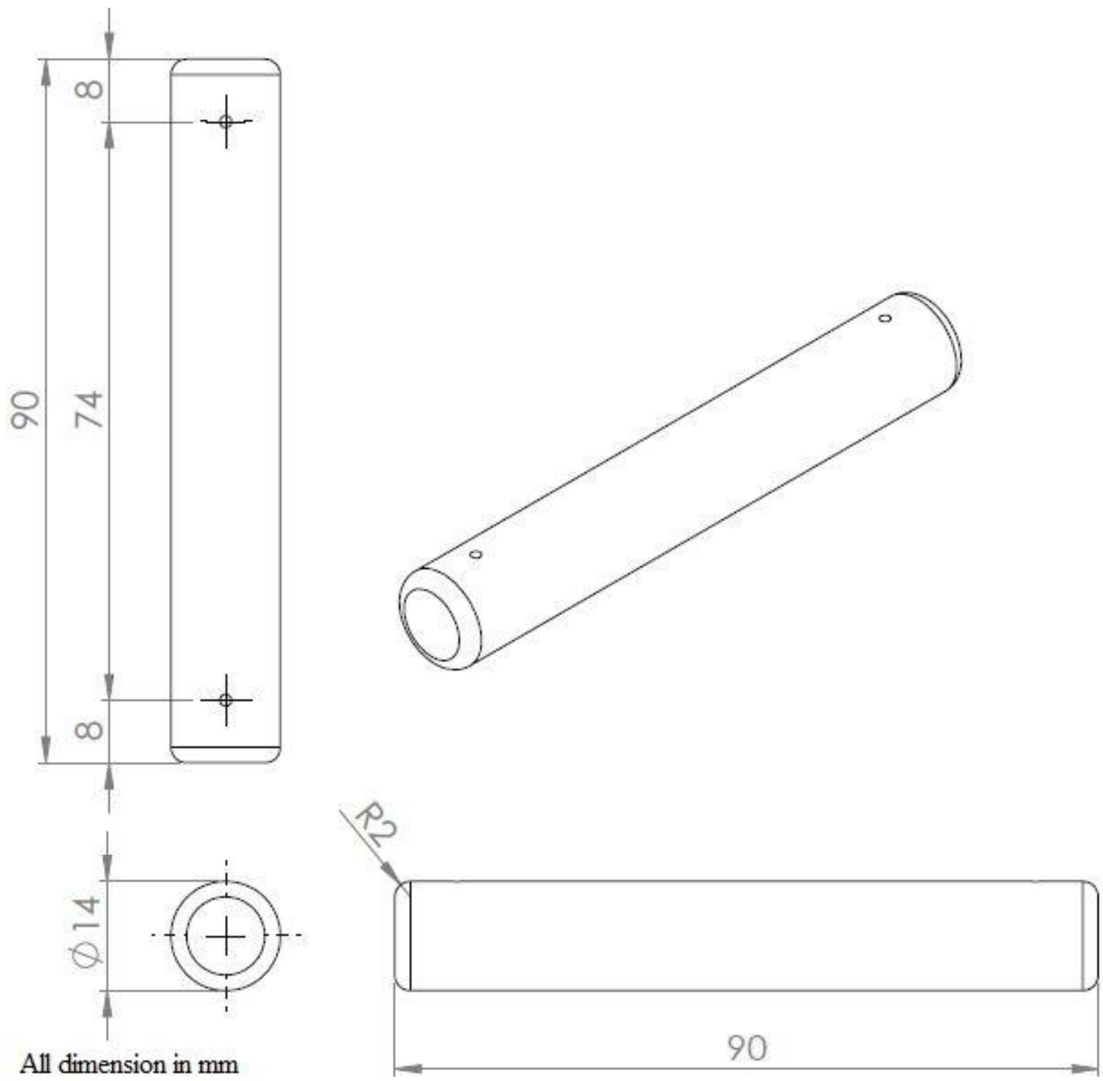

Figure 6.5: Two-dimensional drawing of the pin

APPENDIX B6

DRAWING OF THE ASSAMBLY

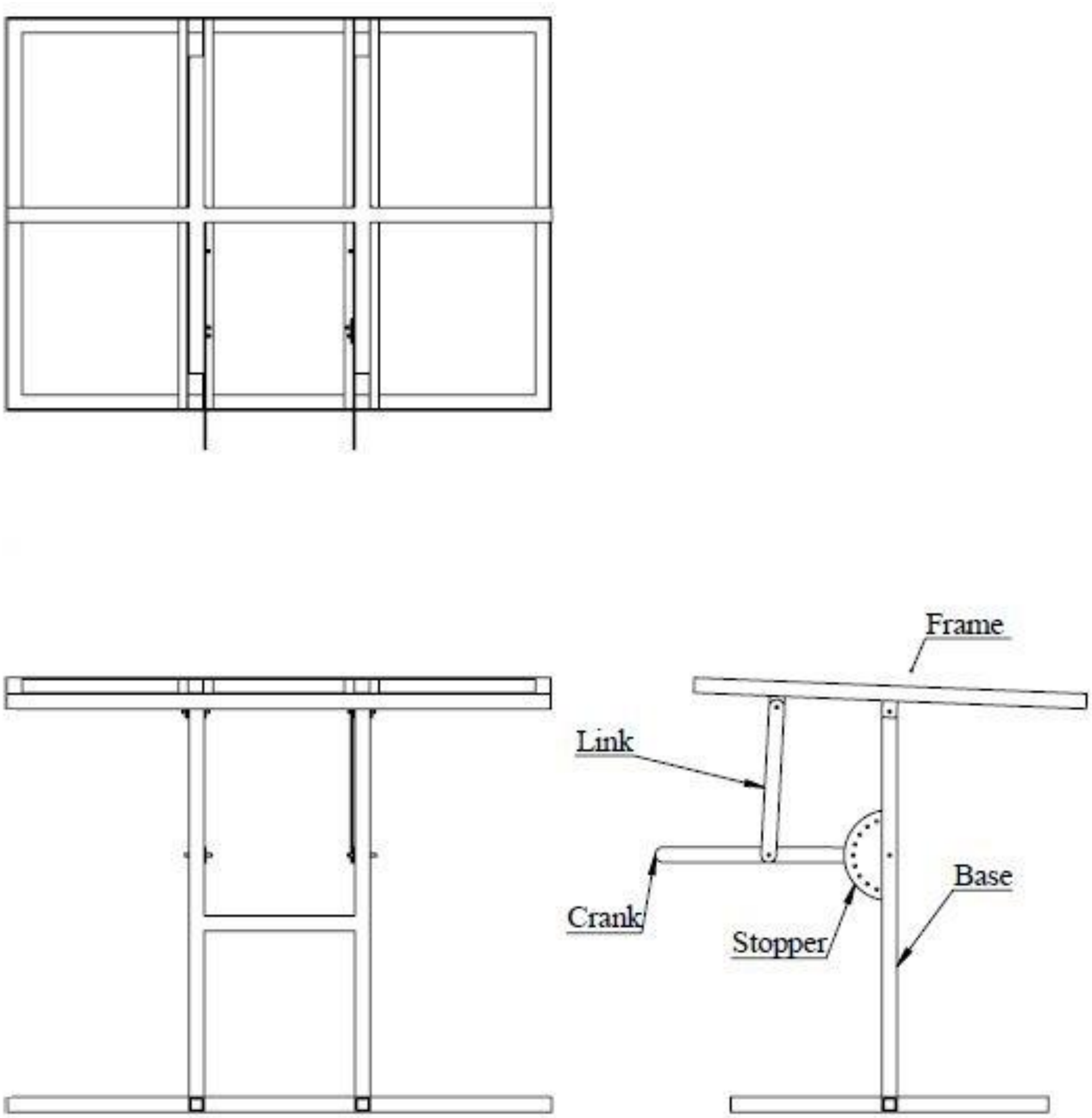

Figure 6.6: Two-dimensional drawing of the assembly part

APPENDIX C1

VON MISES STRESS FOR FRAME

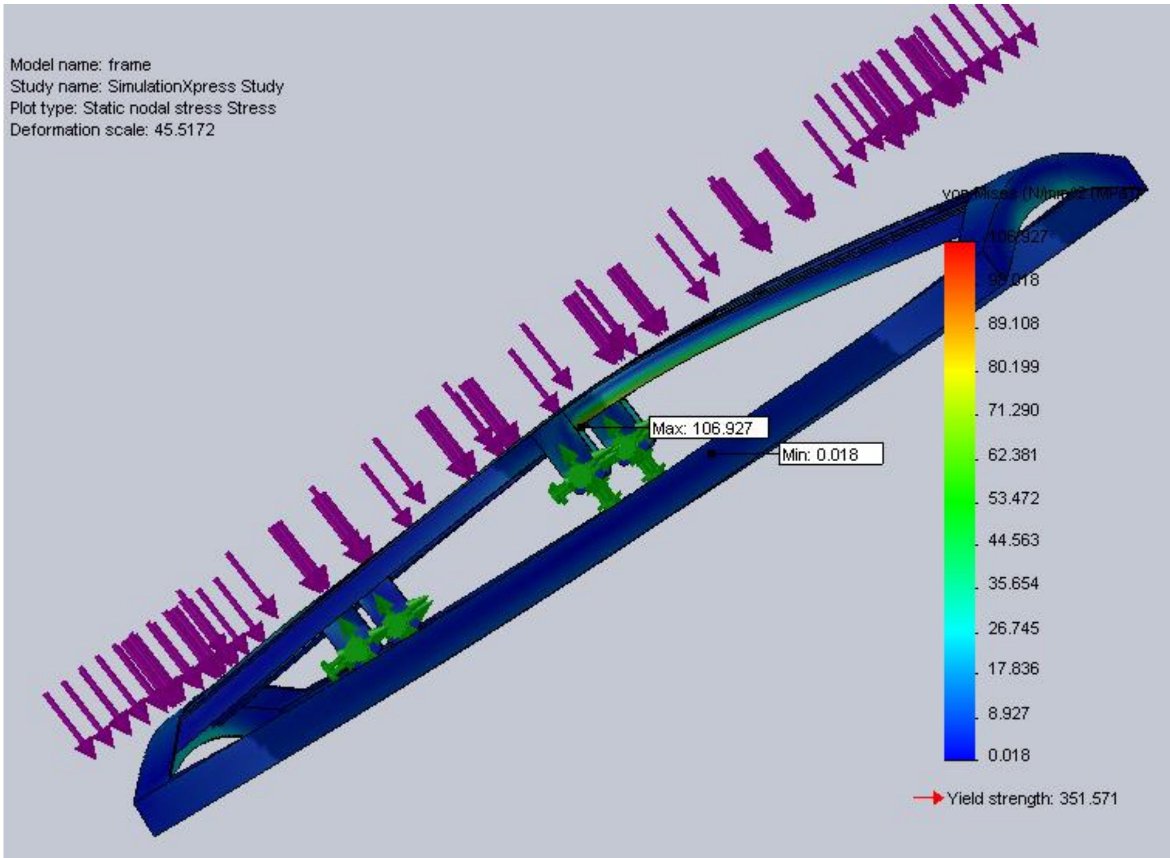

Figure 6.7: The von Mises stress distribution across the frame

APPENDIX C2

VON MISES STRESS FOR LINK

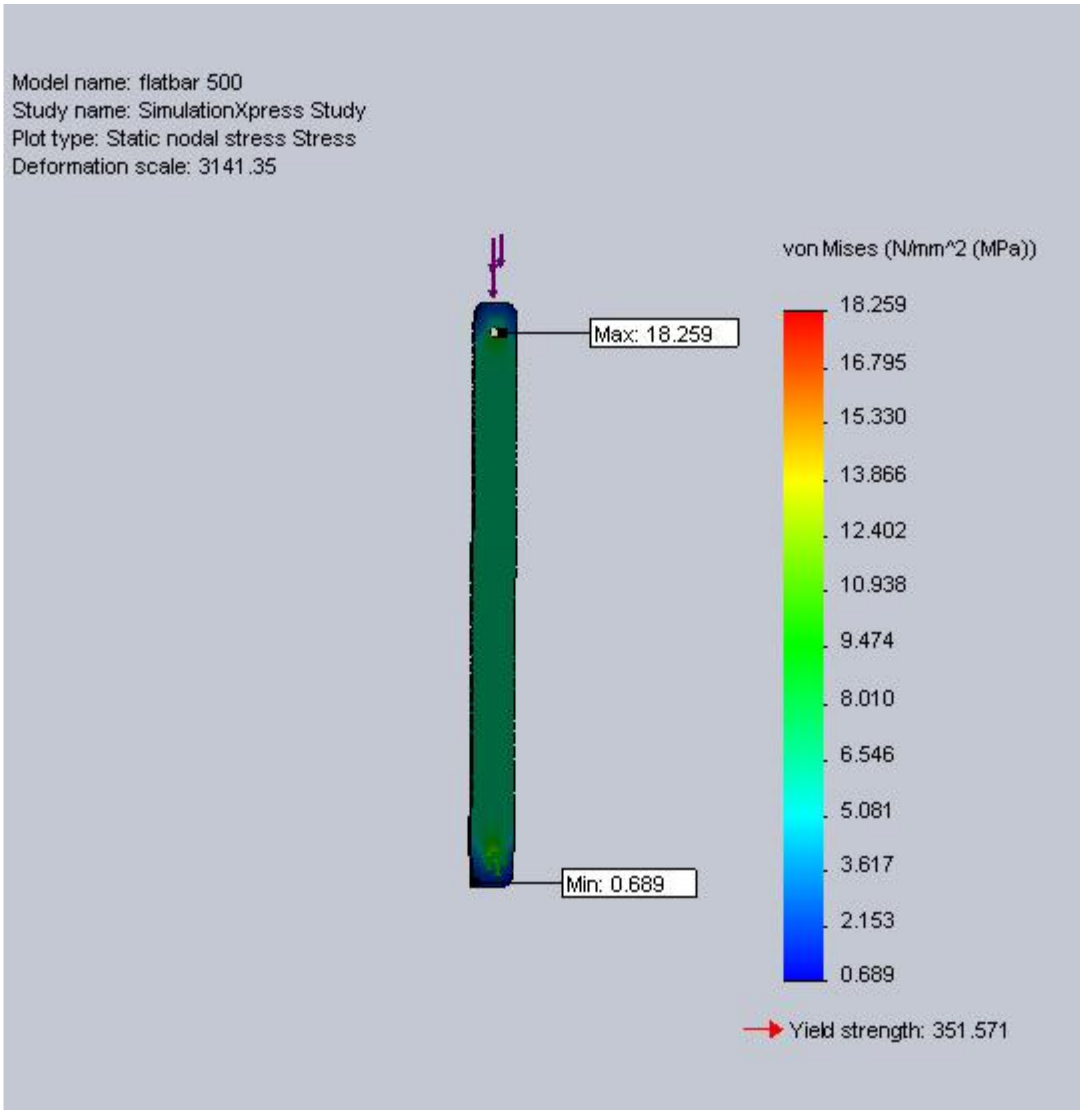

Figure 6.8: The von Mises stress distribution across the link

APPENDIX C3

VON MISES STRESS FOR CRANK

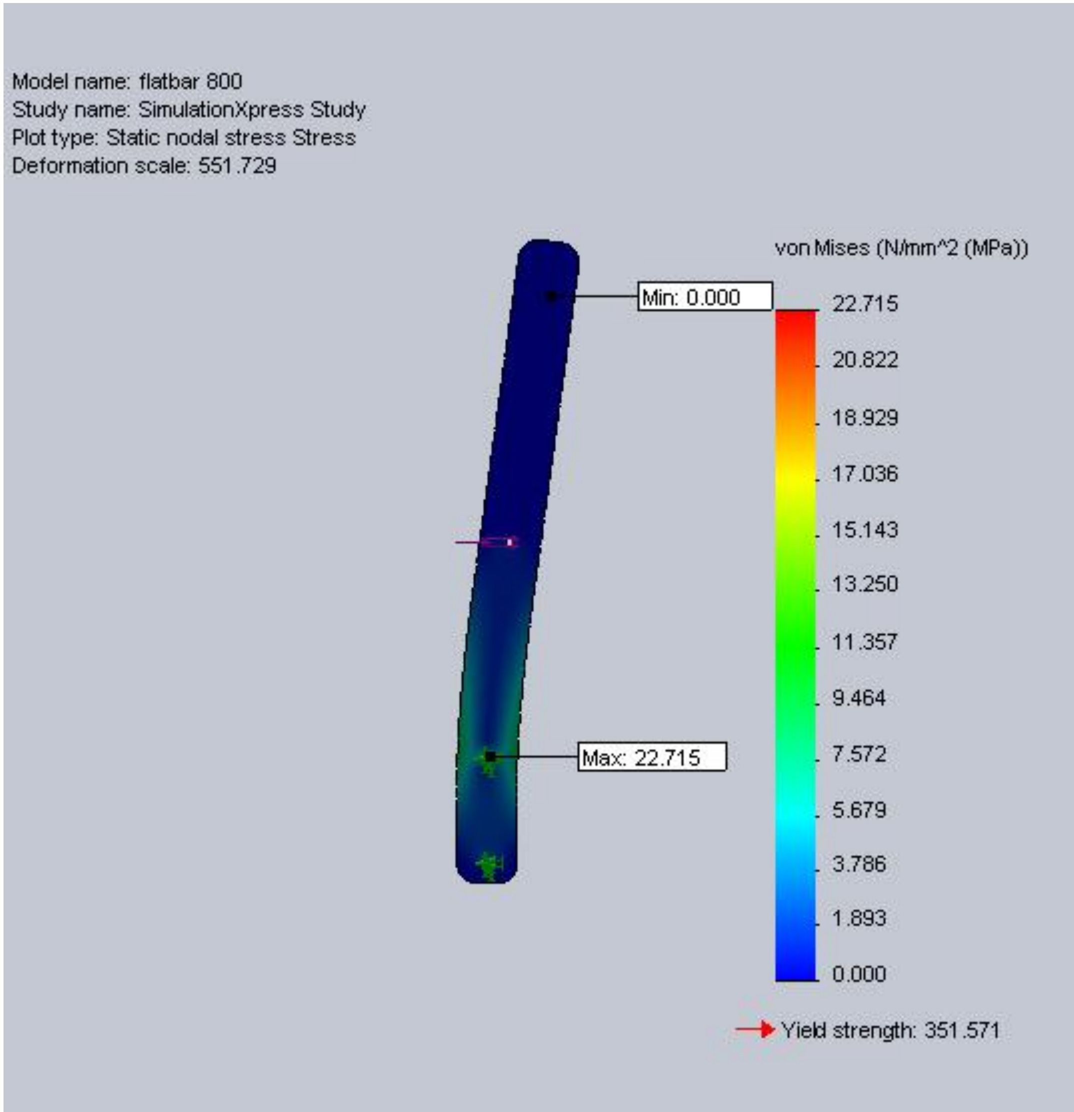

Figure 6.9: The von Mises stress distribution across the crank

APPENDIX C4

VON MISES STRESS FOR BASE

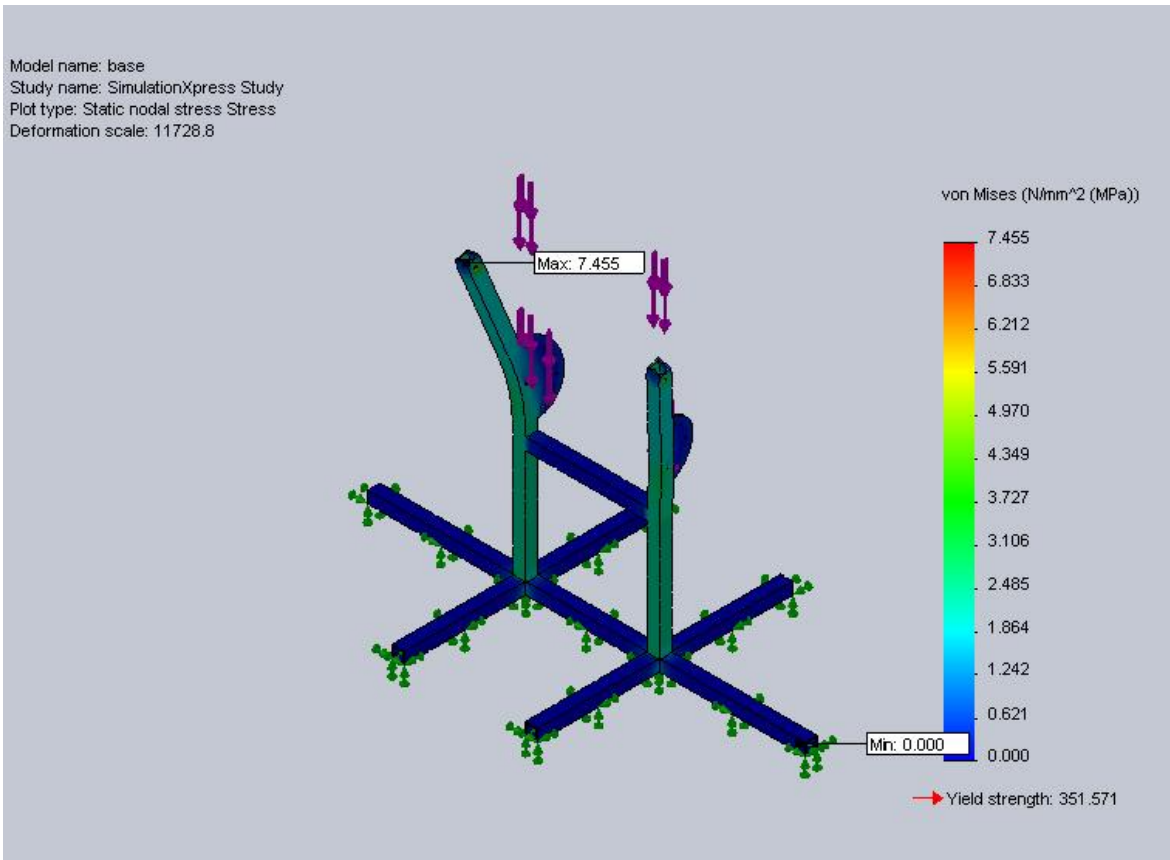

Figure 6.10: The von Mises stress distribution across the base

APPENDIX C5

VON MISES STRESS FOR PIN

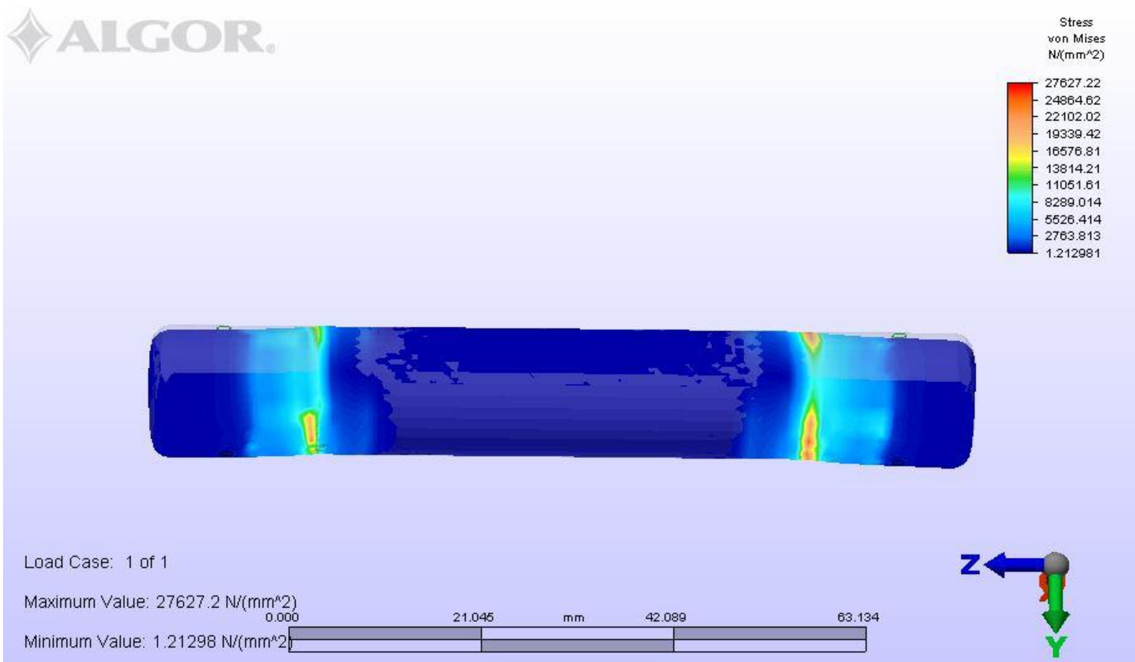

Figure 6.11: The von Mises stress distribution across the pin

APPENDIX D1

SAFETY FACTOR FOR FRAME

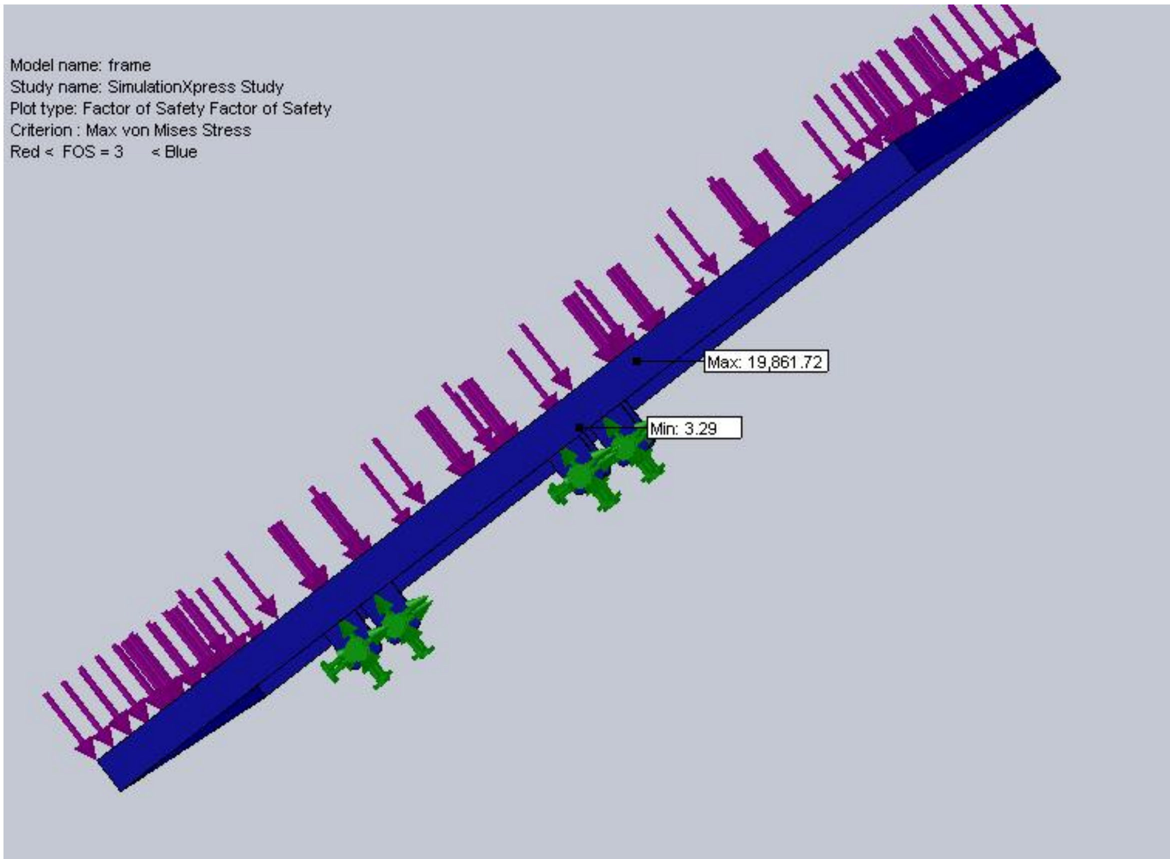

Figure 6.12: The safety factor across the frame

APPENDIX D2

SAFETY FACTOR FOR LINK

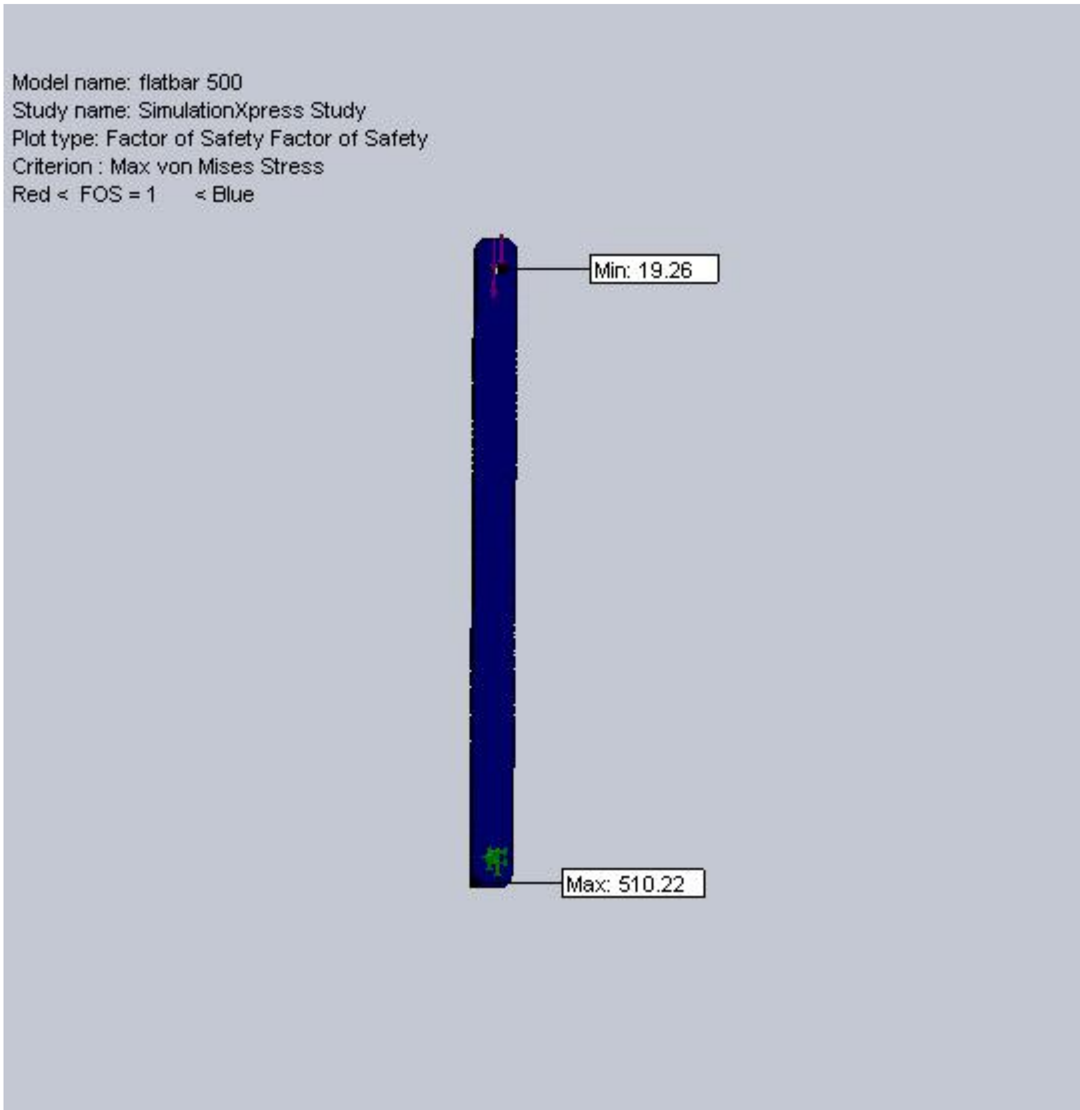

Figure 6.13: The safety factor across the link

APPENDIX D3

SAFETY FACTOR FOR CRANK

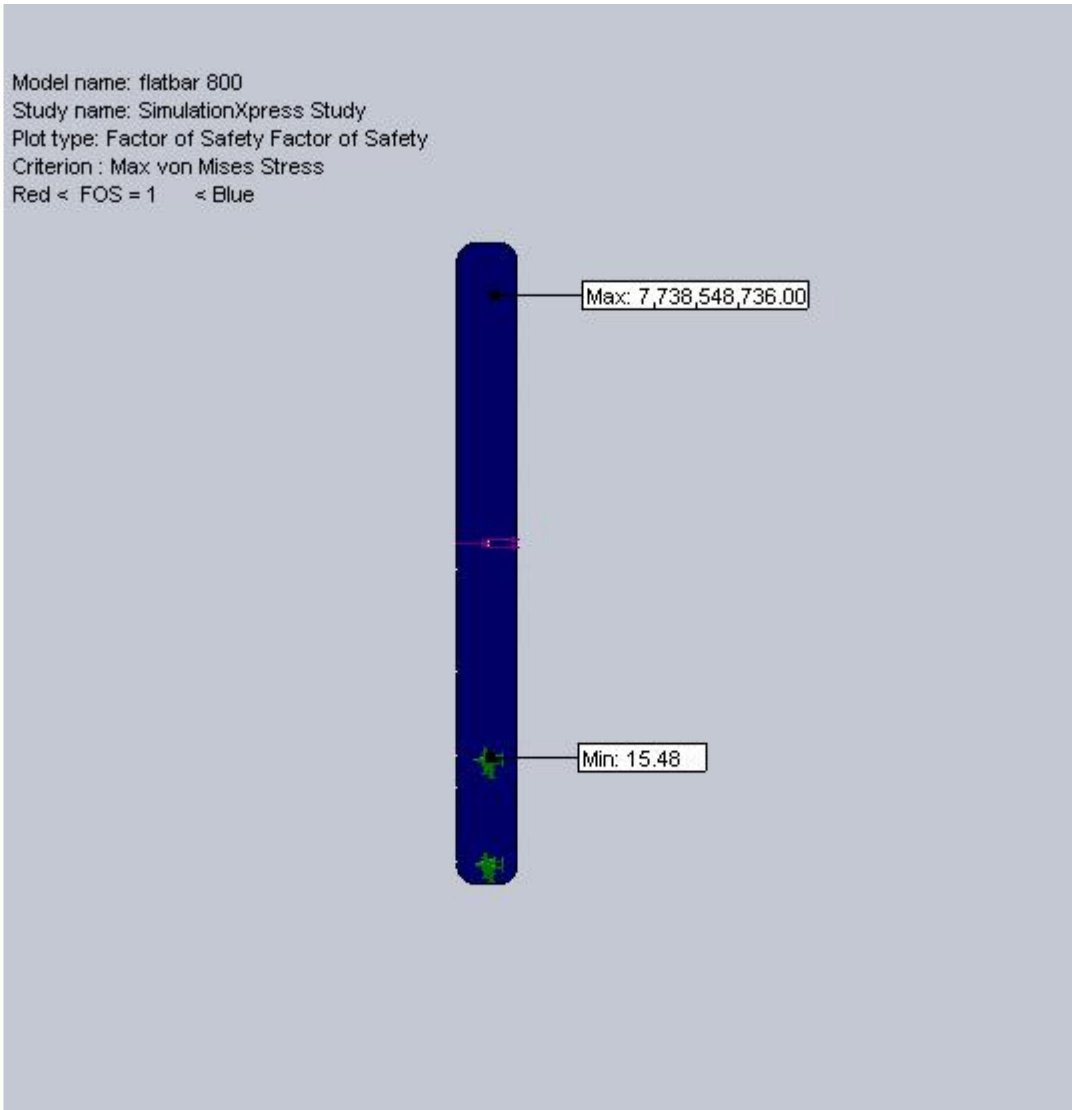

Figure 6.14: The safety factor across the crank

APPENDIX D4

SAFETY FACTOR FOR BASE

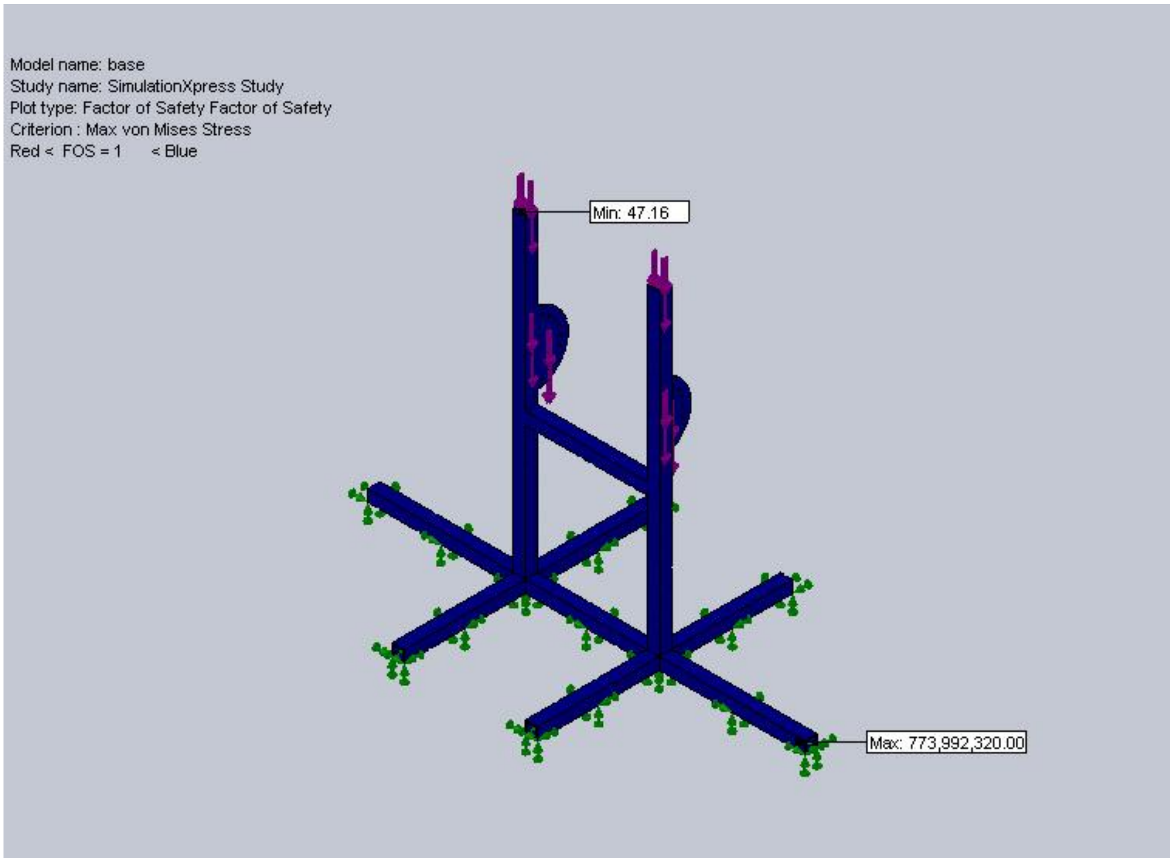

Figure 6.15: The safety factor across the base

APPENDIX D5

SAFETY FACTOR FOR PIN

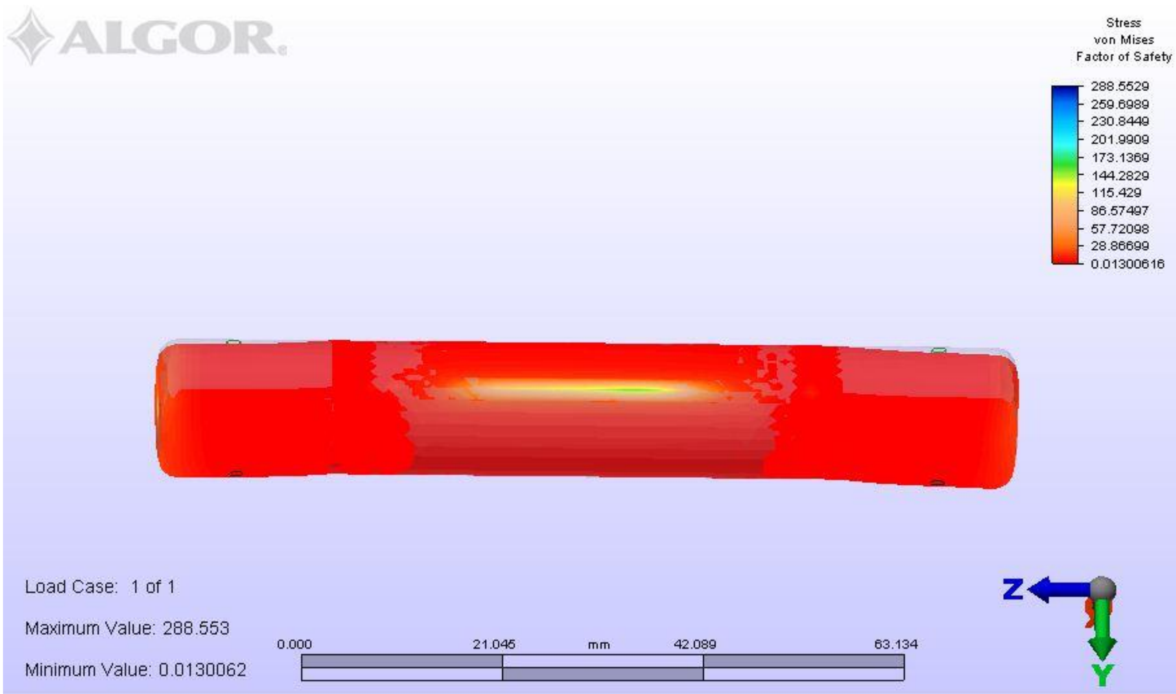

Figure 6.16: The safety factor across the pin

APPENDIX E1

DISPLACEMENT FOR FRAME

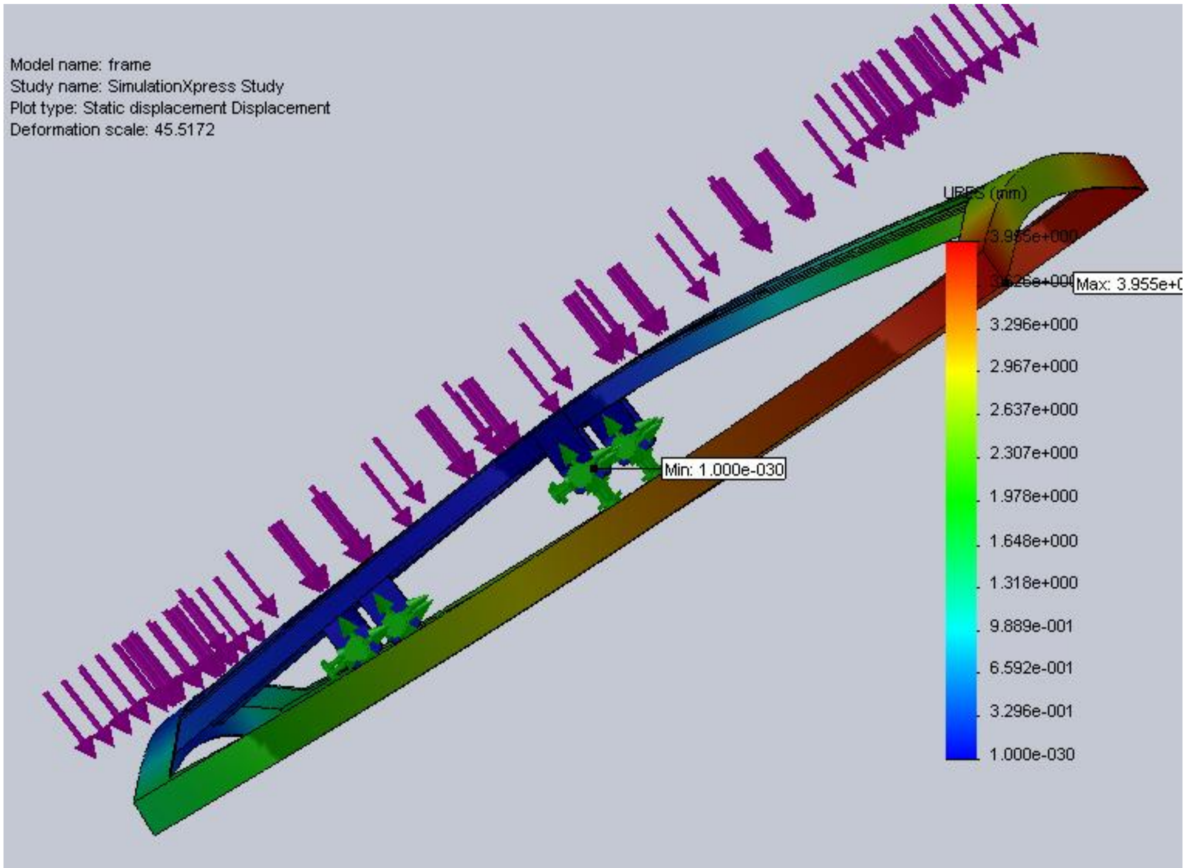

Figure 6.17: Frame displacement under given load

APPENDIX E2

DISPLACEMENT FOR LINK

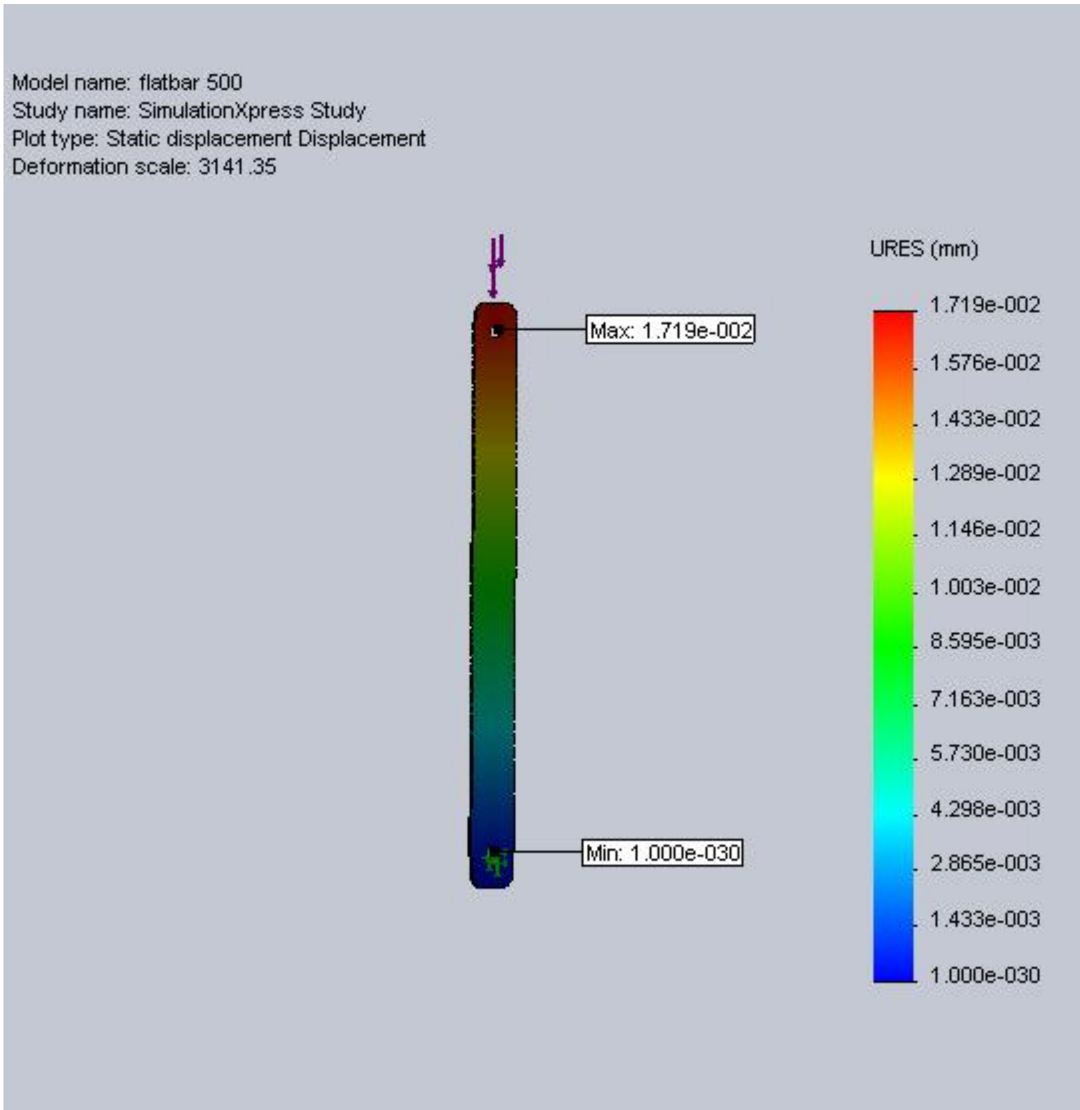

Figure 6.18: Link displacement under given load

APPENDIX E3

DISPLACEMENT FOR CRANK

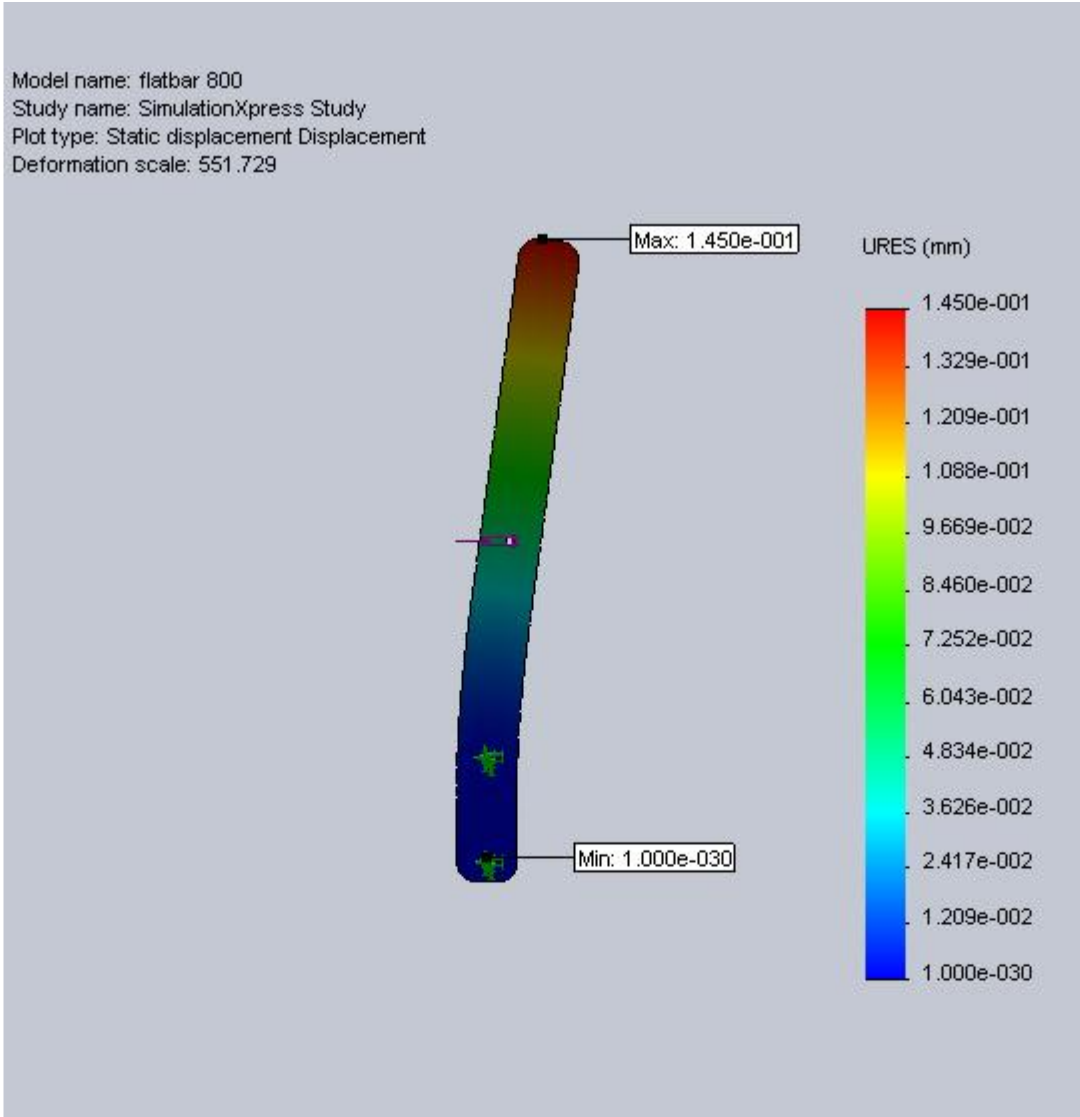

Figure 6.19: Crank displacement under given load

APPENDIX E4

DISPLACEMENT FOR BASE

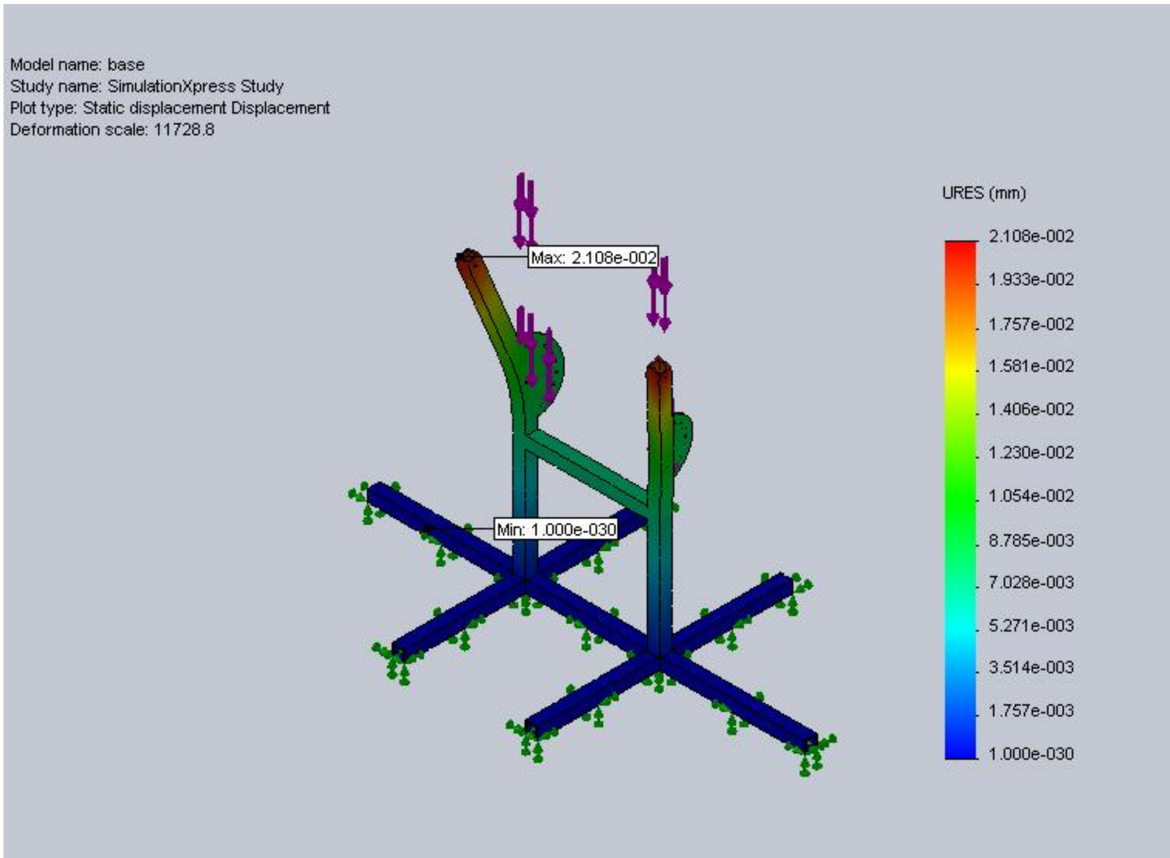

Figure 6.20: Base displacement under given load

APPENDIX E5

DISPLACEMENT FOR PIN

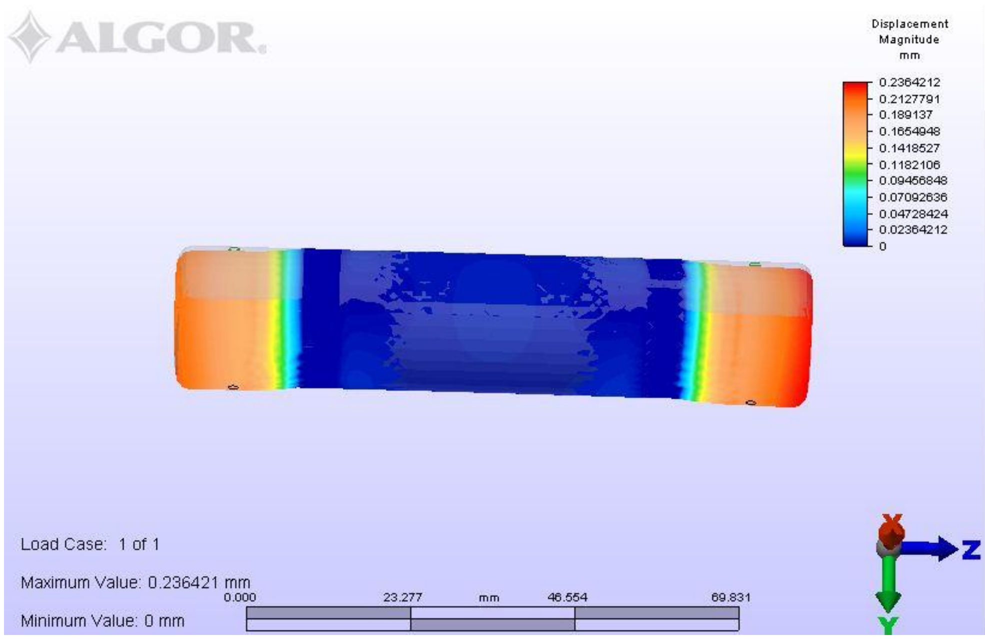

Figure 6.21: Pin displacement under given load